Strike-slip faults

Ramón Arrowsmith
ramon.arrowsmith@asu.edu

School of Earth and Space Exploration
Arizona State University

Outline

- Some basic ideas and definitions to keep in mind
  - Standard model for crustal scale faults
  - Discontinuous strike slip faults
  - Experimental examples to build intuition
- Examples and anecdotes
  - San Andreas Fault tour
  - Alpine Fault, New Zealand
  - Altyn Tagh fault (if time or a future lecture)
- Landscape evolution modeling for intuition

Summary

- Slip rate relative to surface process rates
- Localization ~ slip rate and scale of mapping
- Fault zone discontinuities
- Fault zone orientation relative to drainage network (parallel or perpendicular)
- Degree of (differential) rock uplift along the fault zone: can inset the landscape

Synoptic view of continental shear zone (Scholz, 1988)

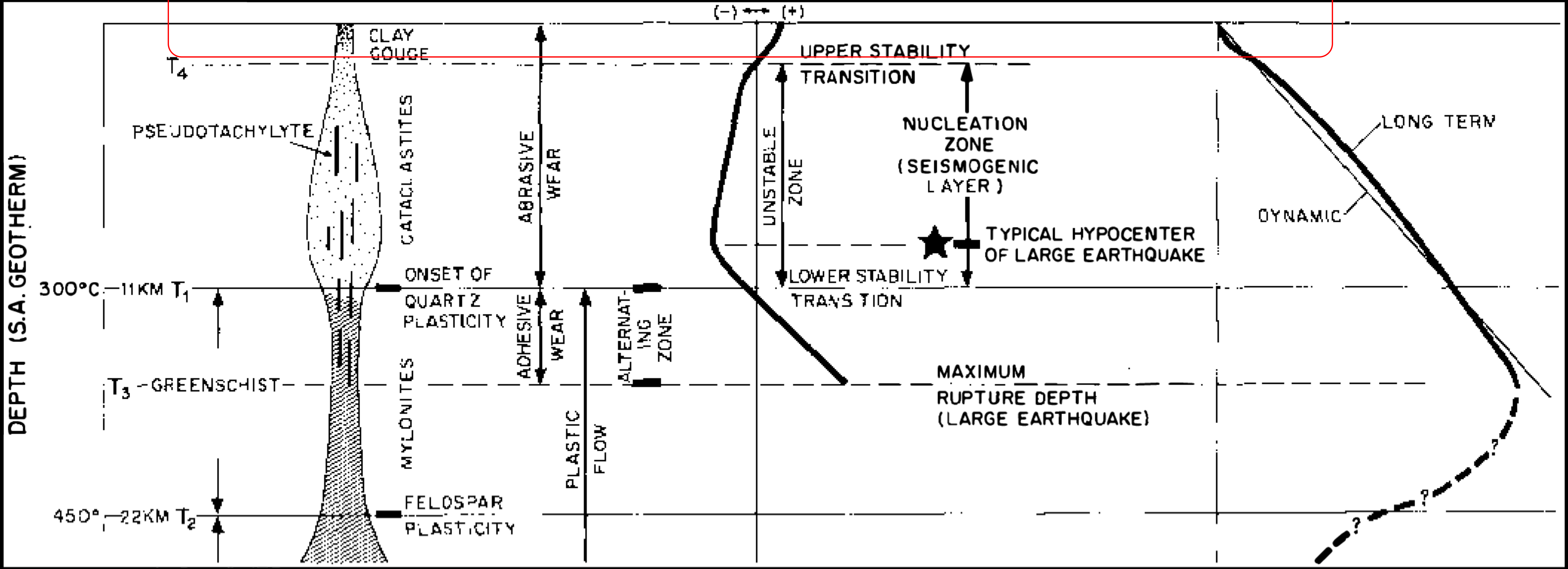

How does the coseismic rupture of the seismogenic layer transmit deformation through the upper stability transition? It is this deformation that drives fault slip and block motion within the shear zone belts that comprise the fault zone at the topographic surface.

Fault zone is comprised of heterogeneous non coplanar fault surfaces bounding oblate blocks whose geometry and activity varies in time and space

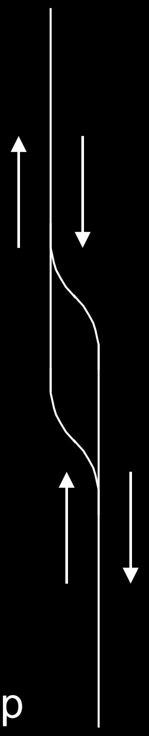

Map view mode II step (bend)

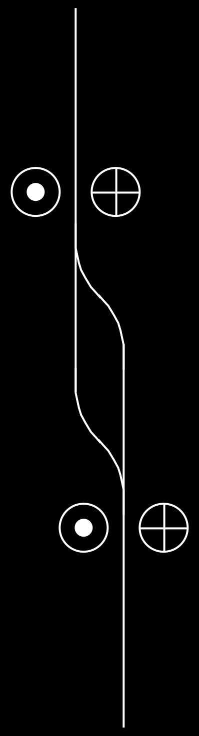

Cross-section view mode III step (bend)

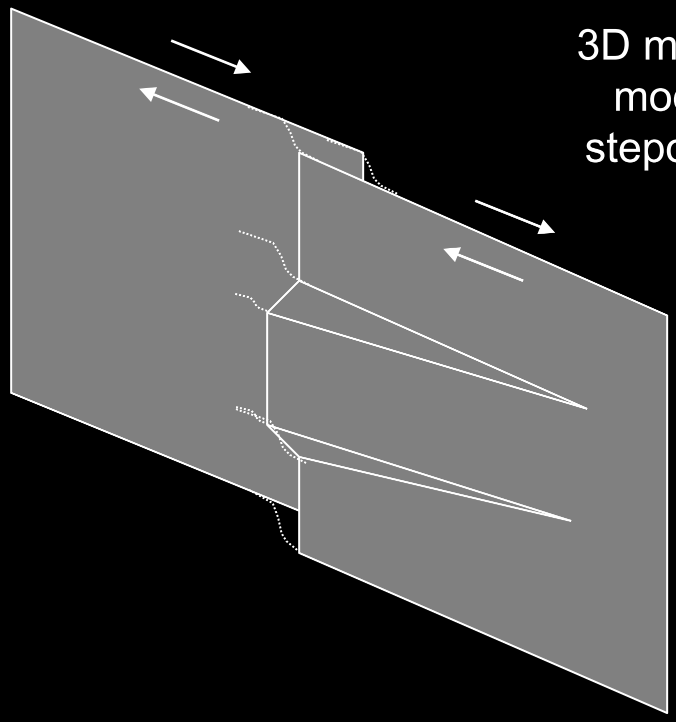

3D mixed mode stepover

Strong influences on
•Stress and displacement fields around the fault surfaces
•Further development and linkage
•Fluid flow
•Rupture dynamics
•Fault zone strength

Questions:
Geometric—Fault surface and block shapes and sizes
Time—How long are they active? What is slip history? Block motion history?
Development—Linkage and evolution of roughness

100 m scale: shear zones

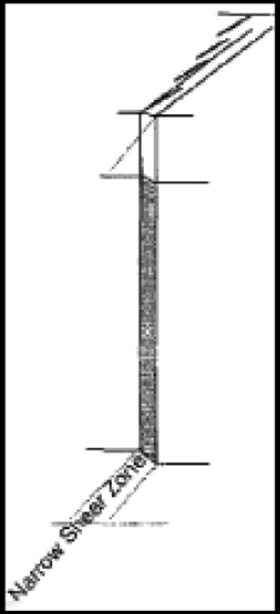

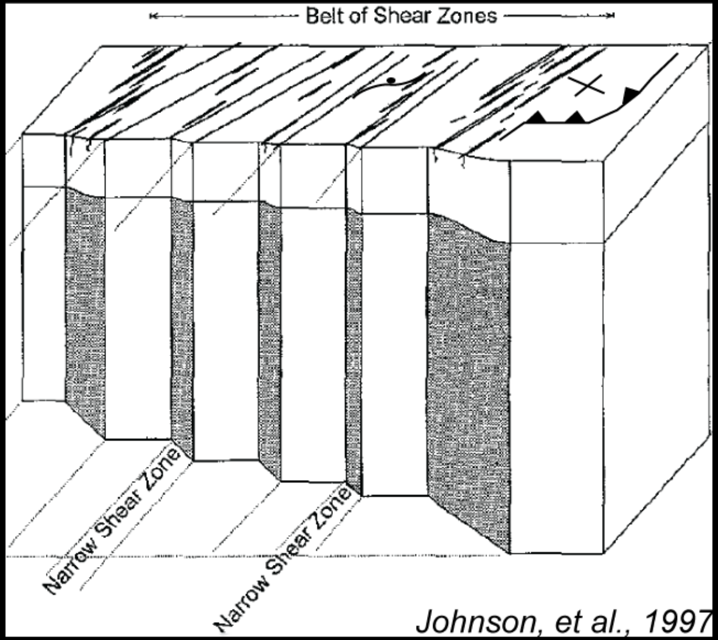

Johnson, et al., 1997

1 km scale: top of FZ

Up through the top of the fault zone: discontinuities, localization, Mode III, and geomorphology

10 km scale: top of FZ

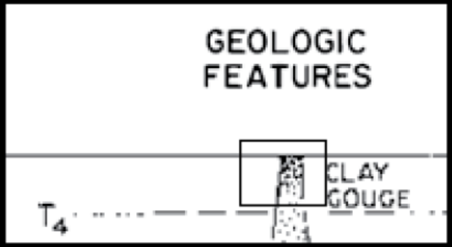

Scholz, 1988

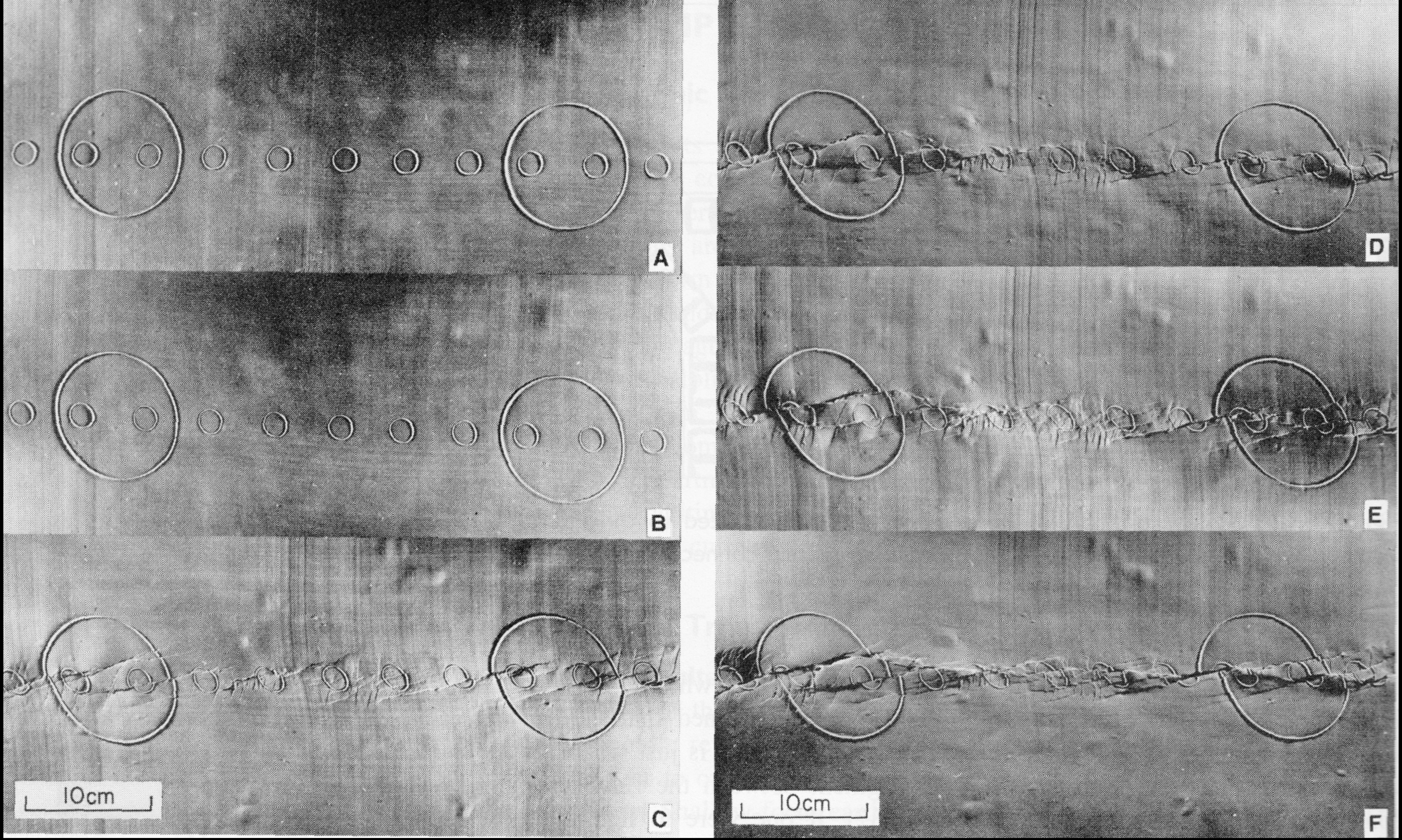

Clay cake experiment simulating strike-slip faulting

-Davis and Reynolds Structural Geology textbook

Strike-slip steps and bends

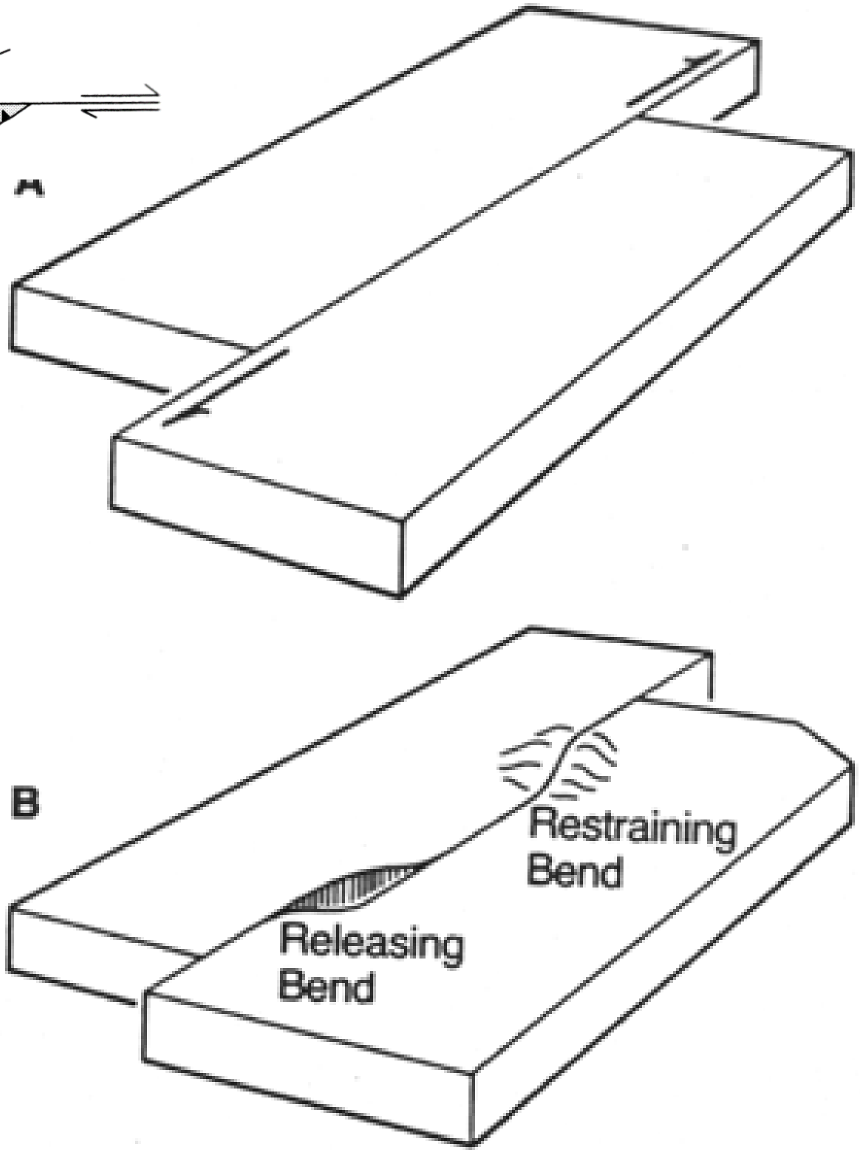

Figure 6.151 (*A*) Strike–slip movement along perfectly planar faults produces neither gaps nor overlaps. (*B*) Strike–slip movement along irregularly curved faults produces gaps at releasing bends and crowding at restraining bends. [From Crowell (1974). Published with permission of Society of Economic Paleontologists and Mineralogists.]

-Davis and Reynolds Structural Geology textbook

Usually one of these traces is the primary trace

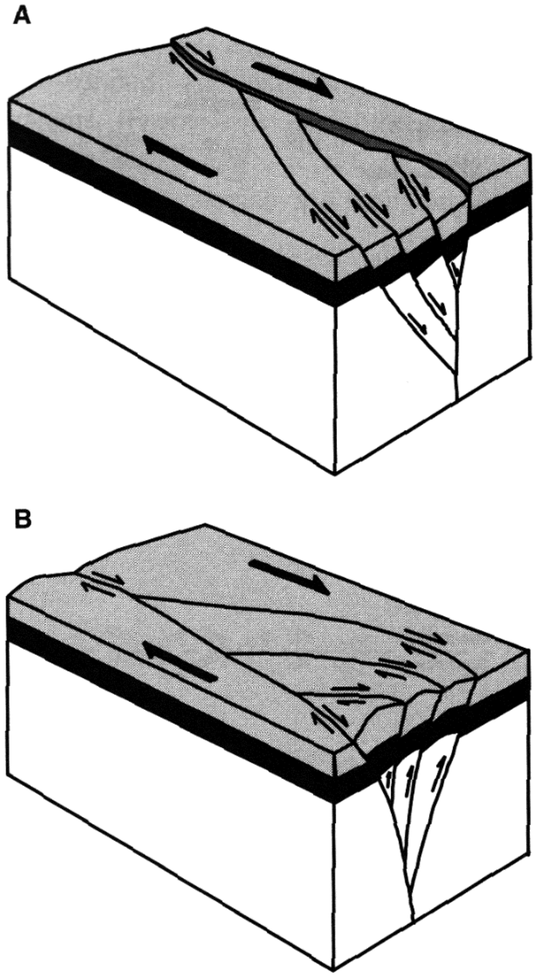

Figure 6.151 Strike-slip duplexes may form at bends along the major strike-slip fault. (*A*) Extensional duplexes form at releasing bends. (*B*) Compressional duplexes form at restraining bends. [From Twiss and Moores, *Structural Geology*, Figs. 7.6 and 7.7, p. 118 and 119. Copyright © 1992, W. H. Freeman and Company, with permission.]

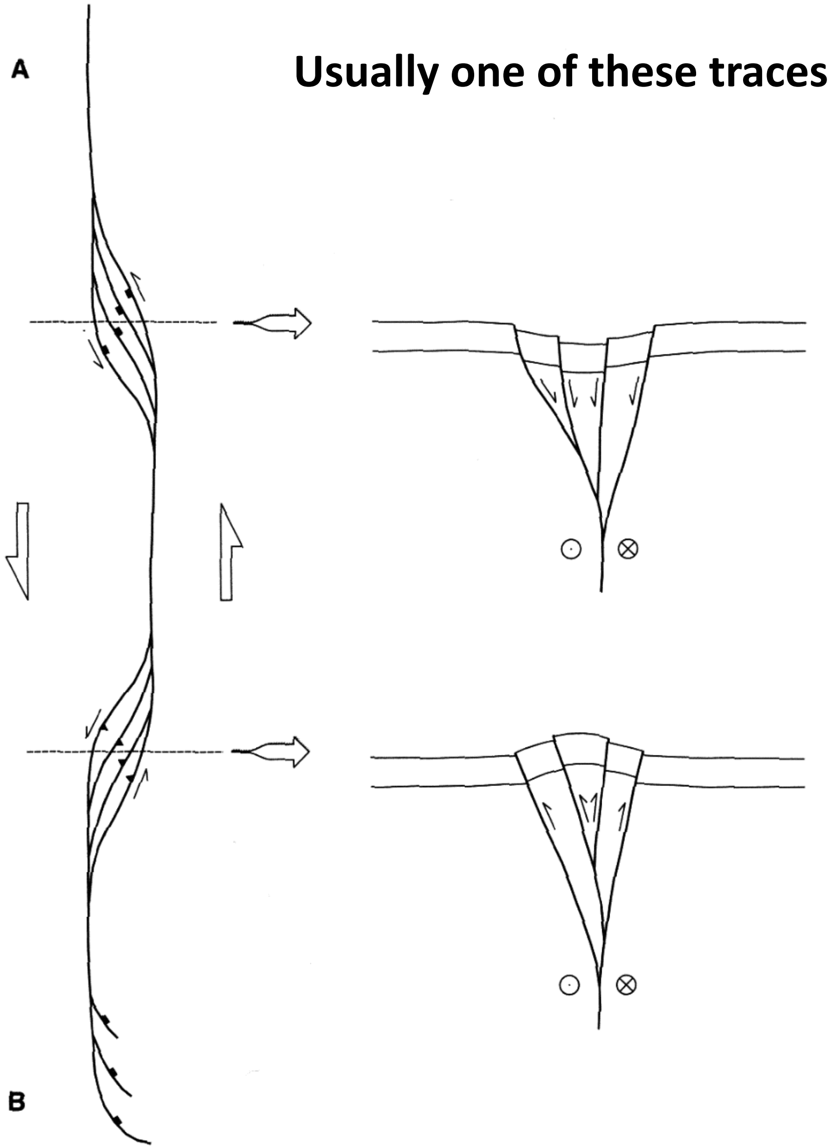

Figure 6.152 (*A*) Map and cross-section of extensional strike-slip duplex at a releasing bend, and the formation of a negative flower structure. (*B*) Map and cross-section of contractional strike-slip duplex at a restraining bend and the formation of a positive flower structure. [Reprinted from *Journal of Structural Geology*, v. 25, Woodcock, N. H., and Rickards, B., Transpressive duplex and flower structure: Dent Fault System, NW England, p. 1981–1992, © 2003, with permission from Elsevier.]

-Davis and Reynolds Structural Geology textbook

San Andreas Fault tour in digital terrain model hillshades: https://www.youtube.com/playlist?list=PLFfZSFyNZ_jZm86F1TsnYfuuYNef_Uh21

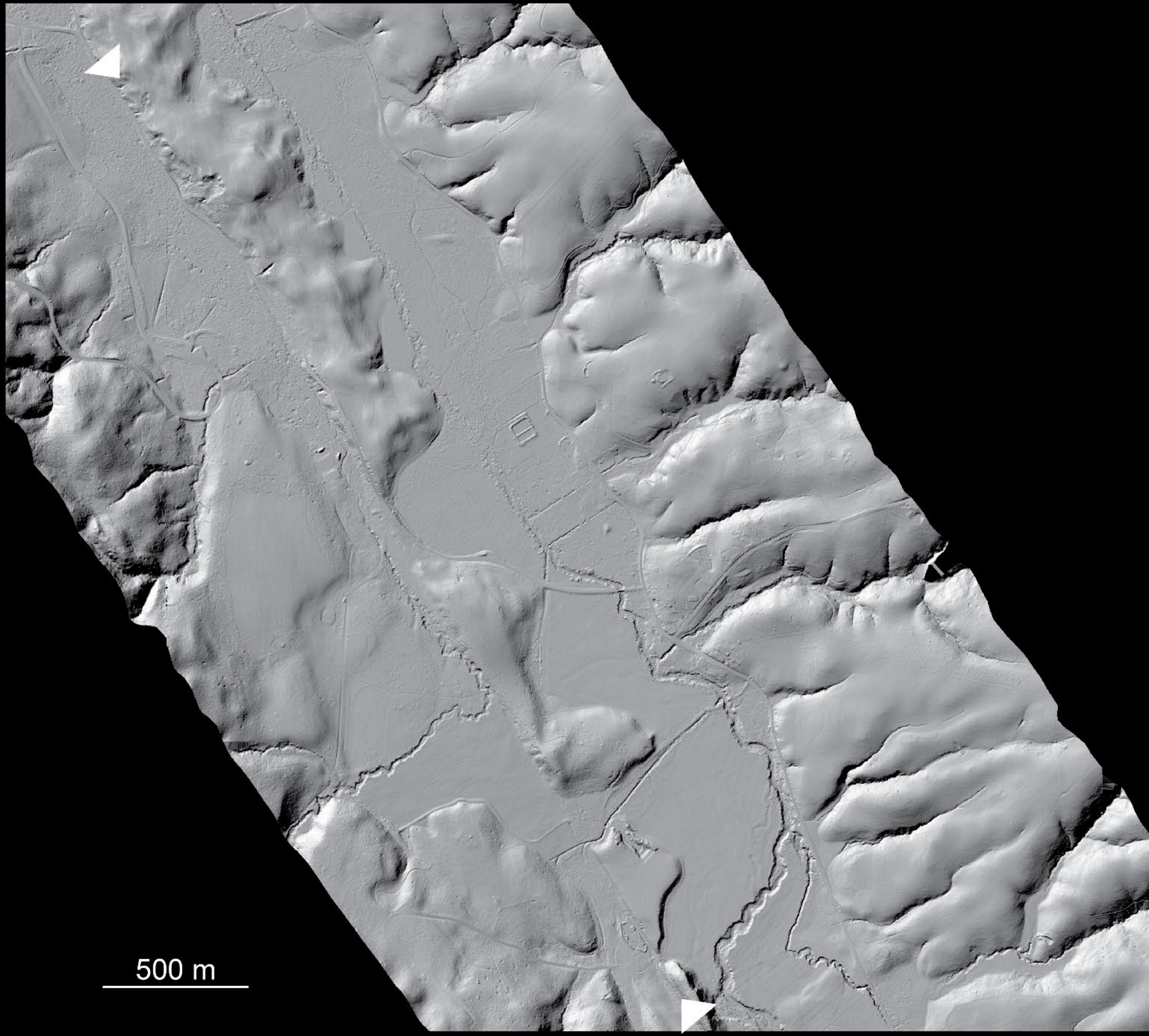

https://fromtheprow.agu.org/remembering-the-great-1906-san-francisco-earthquake/

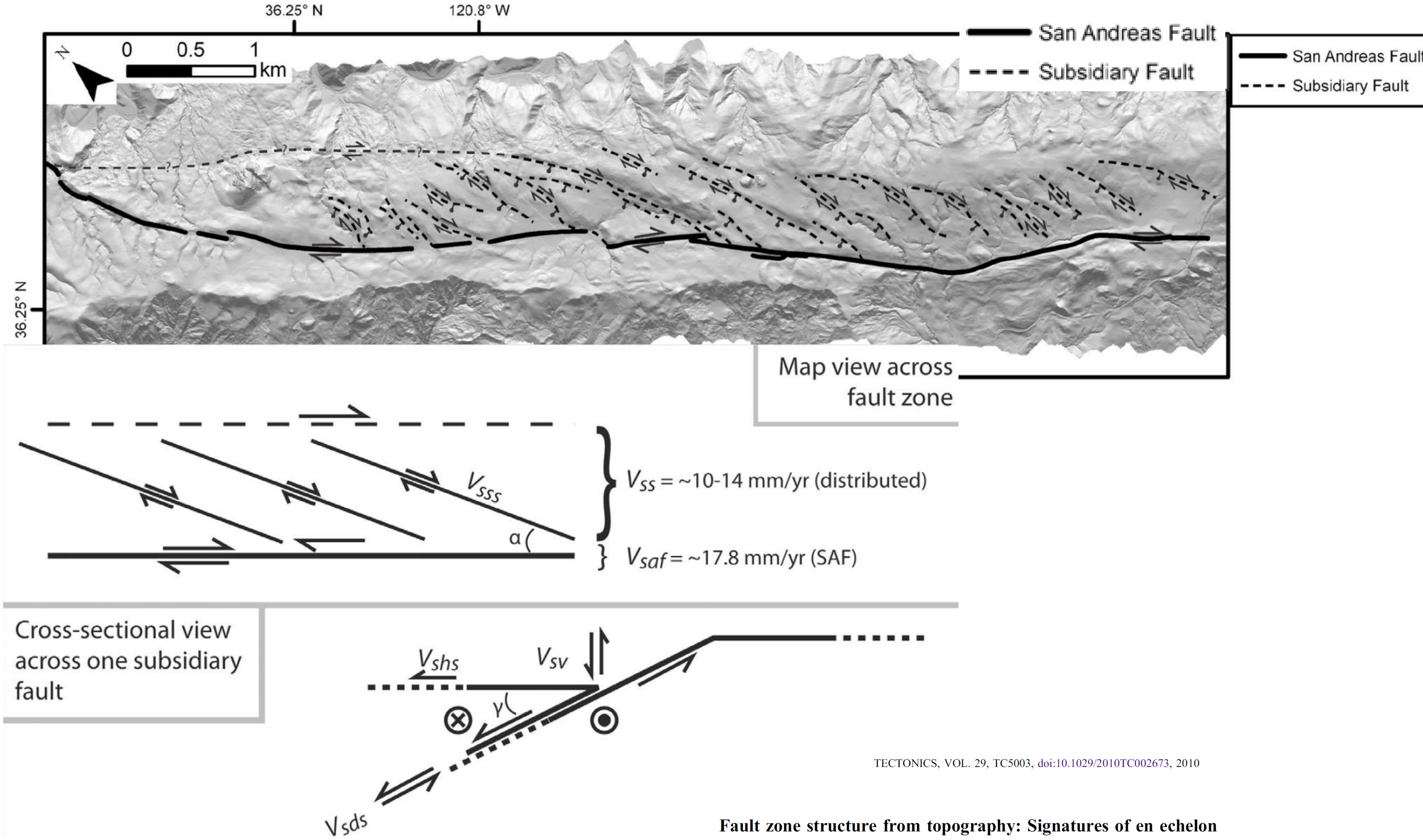

TECTONICS, VOL. 29, TC5003, doi:10.1029/2010TC002673, 2010

Fault zone structure from topography: Signatures of en echelon fault slip at Mustang Ridge on the San Andreas Fault, Monterey County, California

Stephen B. DeLong,[1] George E. Hilley,[2] Michael J. Rymer,[1] and Carol Prentice[1]

Mapping active fault traces

Classic, field, and virtual LiDAR views

An example from the Cholame section of the San Andreas Fault
Arrowsmith and Zielke, 2009

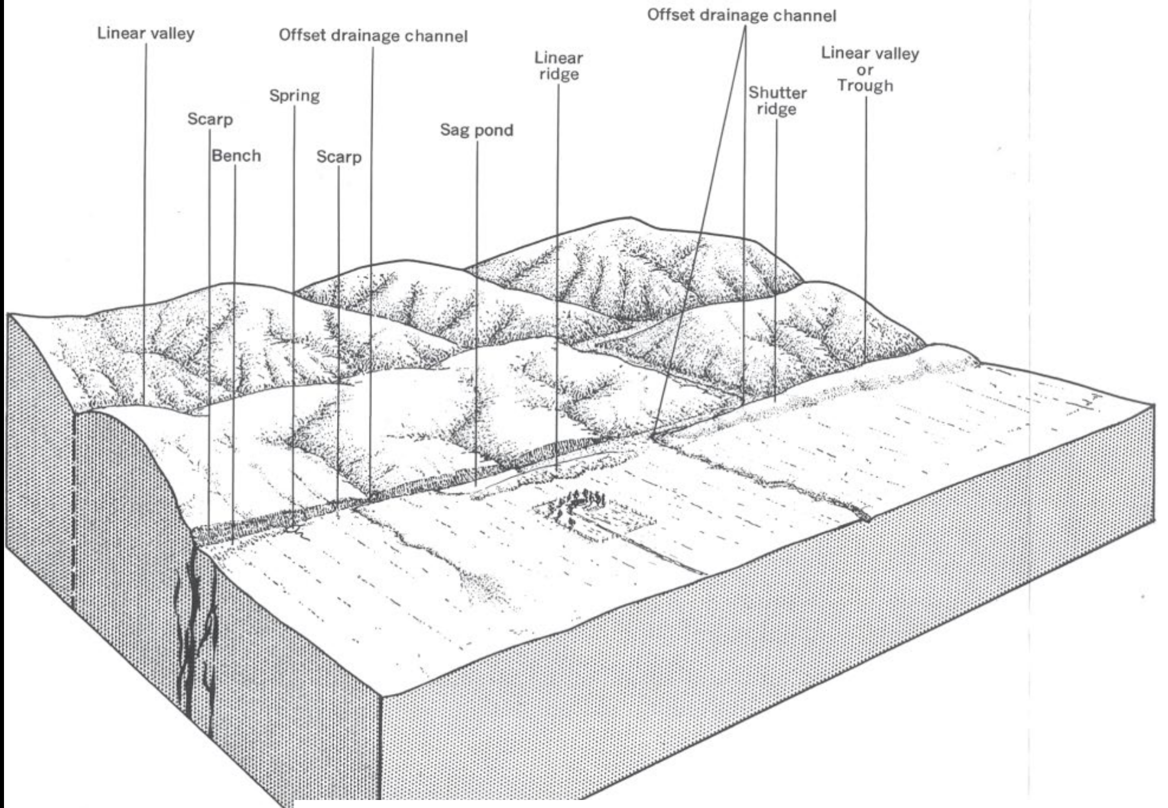

Vedder and Wallace, 1970 and numerous others

Explanation for fault strip mapping

Vedder and Wallace, 1970

- ● Local features with annotation
- Regional features (solid line)
- Recently active breaks, certain (solid red line)
- Recently active breaks, less obvious (dashed red line)
- Ponds and lakes (pink box)

Stone and Arrowsmith

- Fault trace (solid red line)
- Fault trace, concealed (dotted red line)
- Fault trace, inferred (dashed red line)
- Lineament (thin red line)
- Landslide deposit (brown box)
- Landslide scarp (outlined box)
- Sag (blue box)

Zielke, this study

Fault traces: red for main trace, blue for secondary traces

- Fault trace, certain (solid red line)
- Fault trace, inferred (dashed red line)
- ? Fault trace, queried
- Fault trace, uncertain (dotted red line)
- Landslide deposit and scarp (brown box)

Arrowsmith and Zielke, 2009

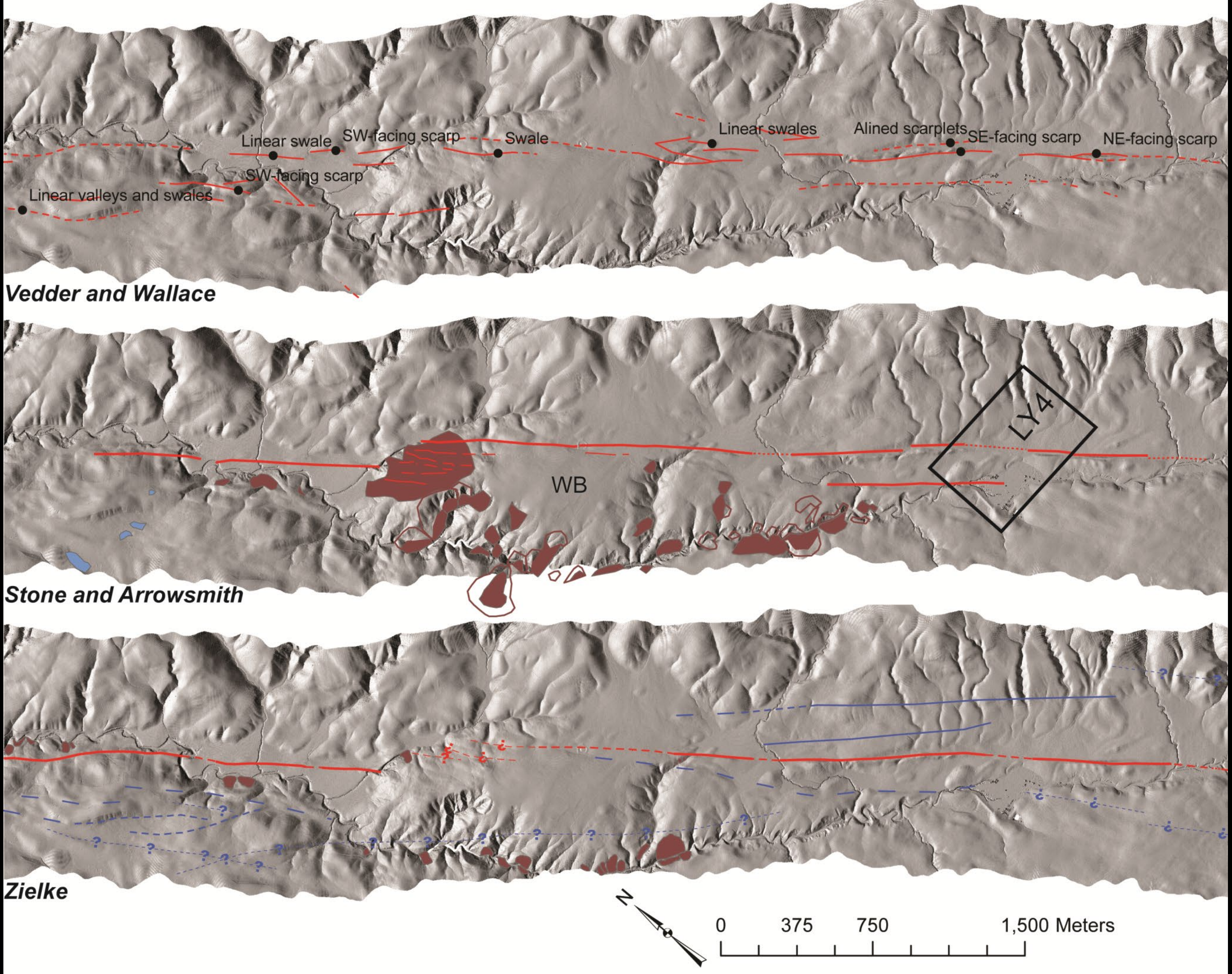

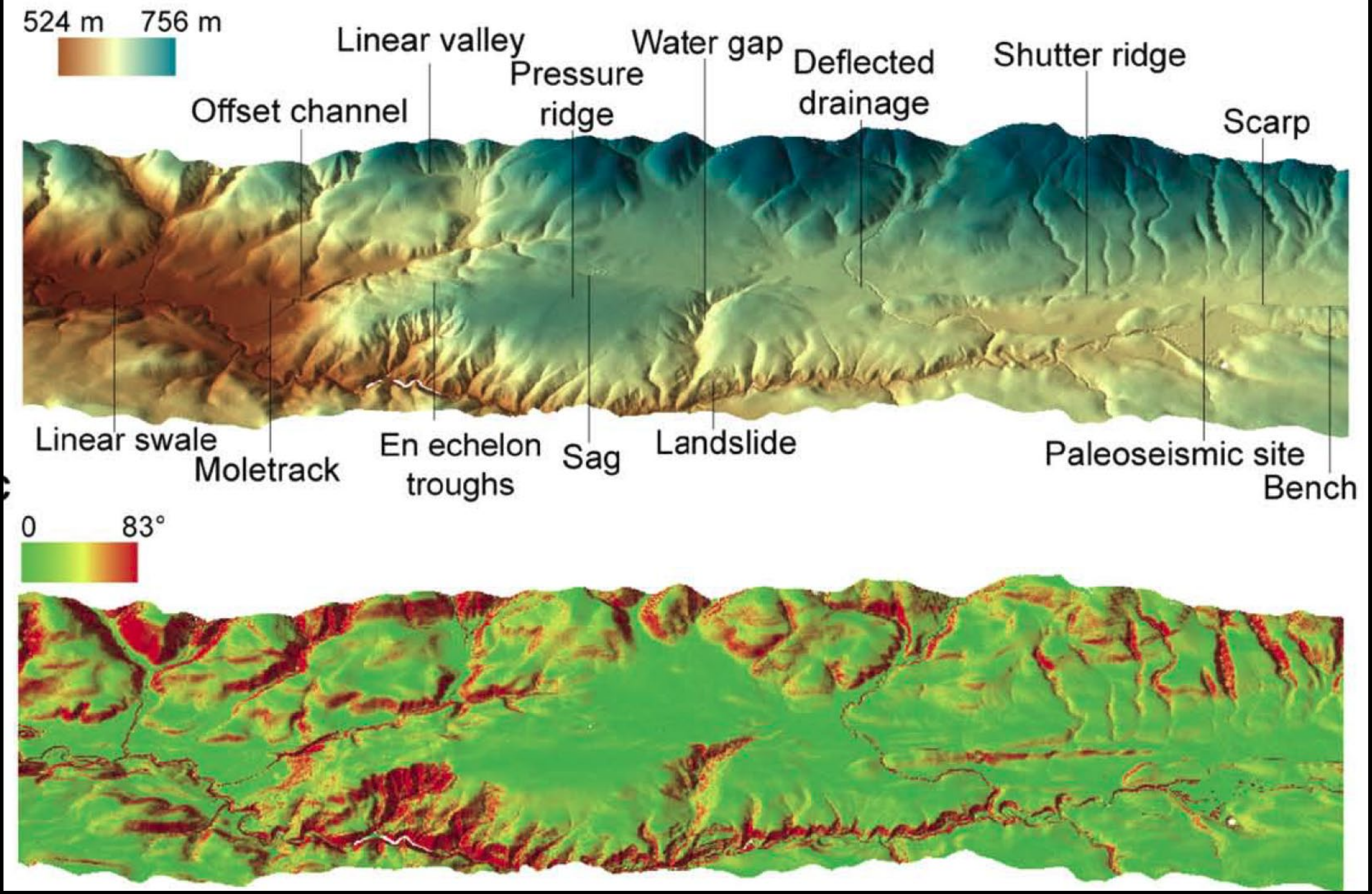

Arrowsmith and Zielke, 2009

Common landforms produced along recently active strike-slip faults such as the south-central San Andreas Fault

Sag ponds along strike-slip faults typically occupy structural depressions created by transtension and normal faulting, which are found in minor releasing steps or bends (e.g., the Pallett Creek and Glen Ivy Marsh sites on the San Andreas fault, California). Such features are readily observed on aerial photographs. More rarely, sediments are trapped when shutter ridges partially or completely block ephemeral drainages that flow perpendicular to fault strike, creating marshes or swamps (e.g., Hall, 1984). Alluvial fan deposition in the fault zone can also block fault-parallel drainage and create marshes.

Sag pond along Creeping San Andreas Fault

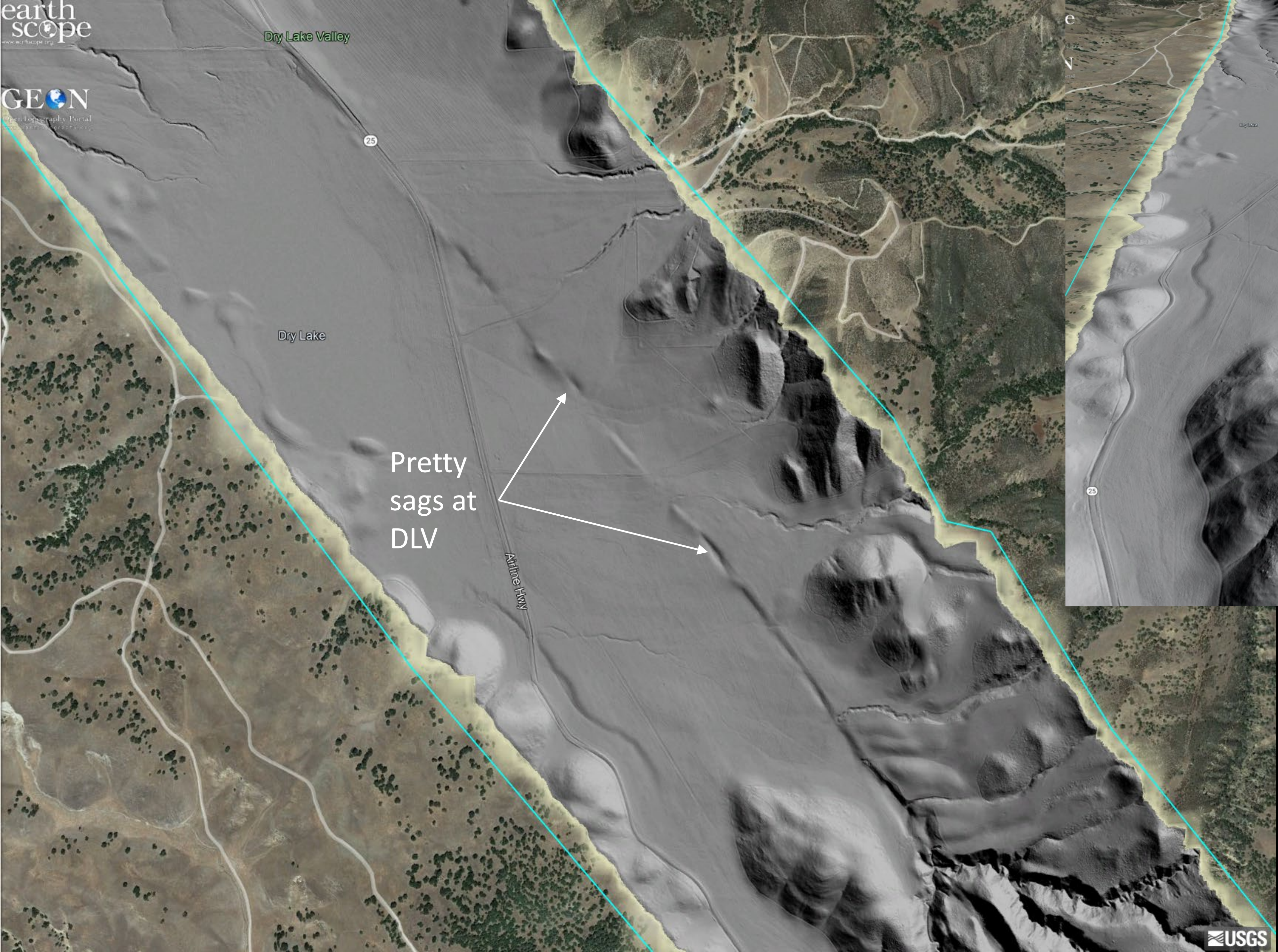

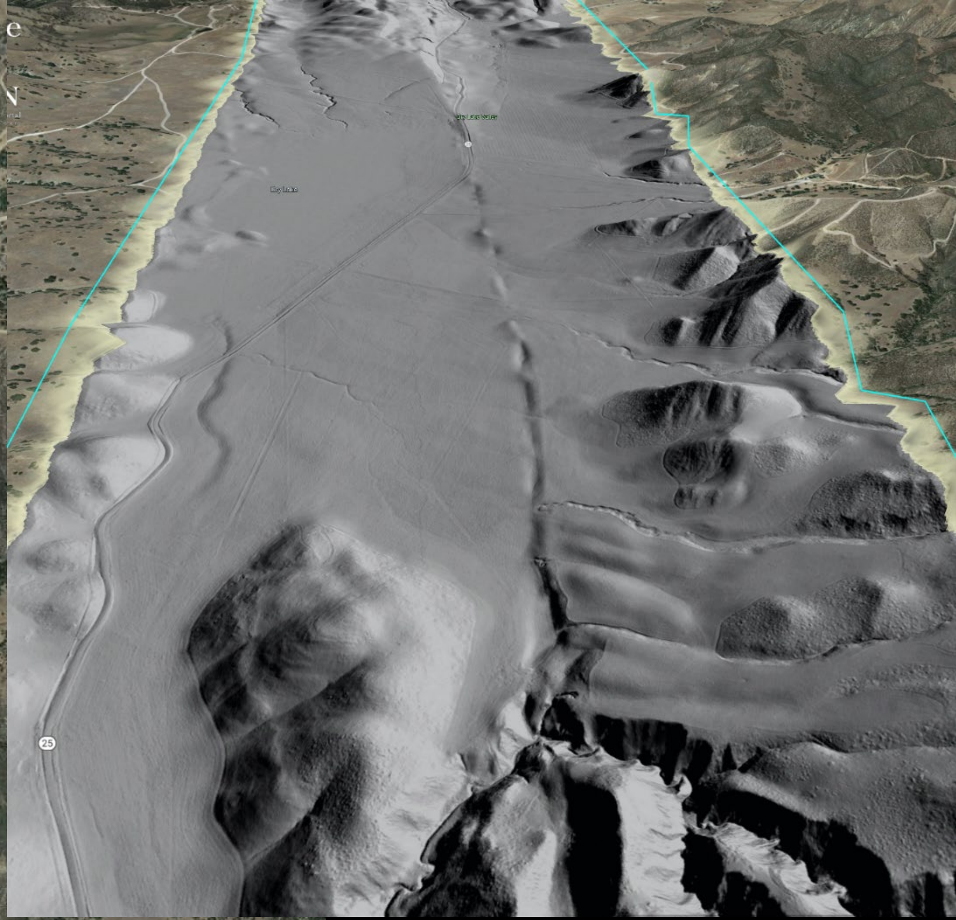

c.f., Scott, C., Bunds, M., Shirzaei, M., & Toke, N. (2020). Creep along the Central San Andreas Fault from surface fractures, topographic differencing, and InSAR. Journal of Geophysical Research: Solid Earth, 125, e2020JB019762. https://doi.org/10.1029/2020JB019762

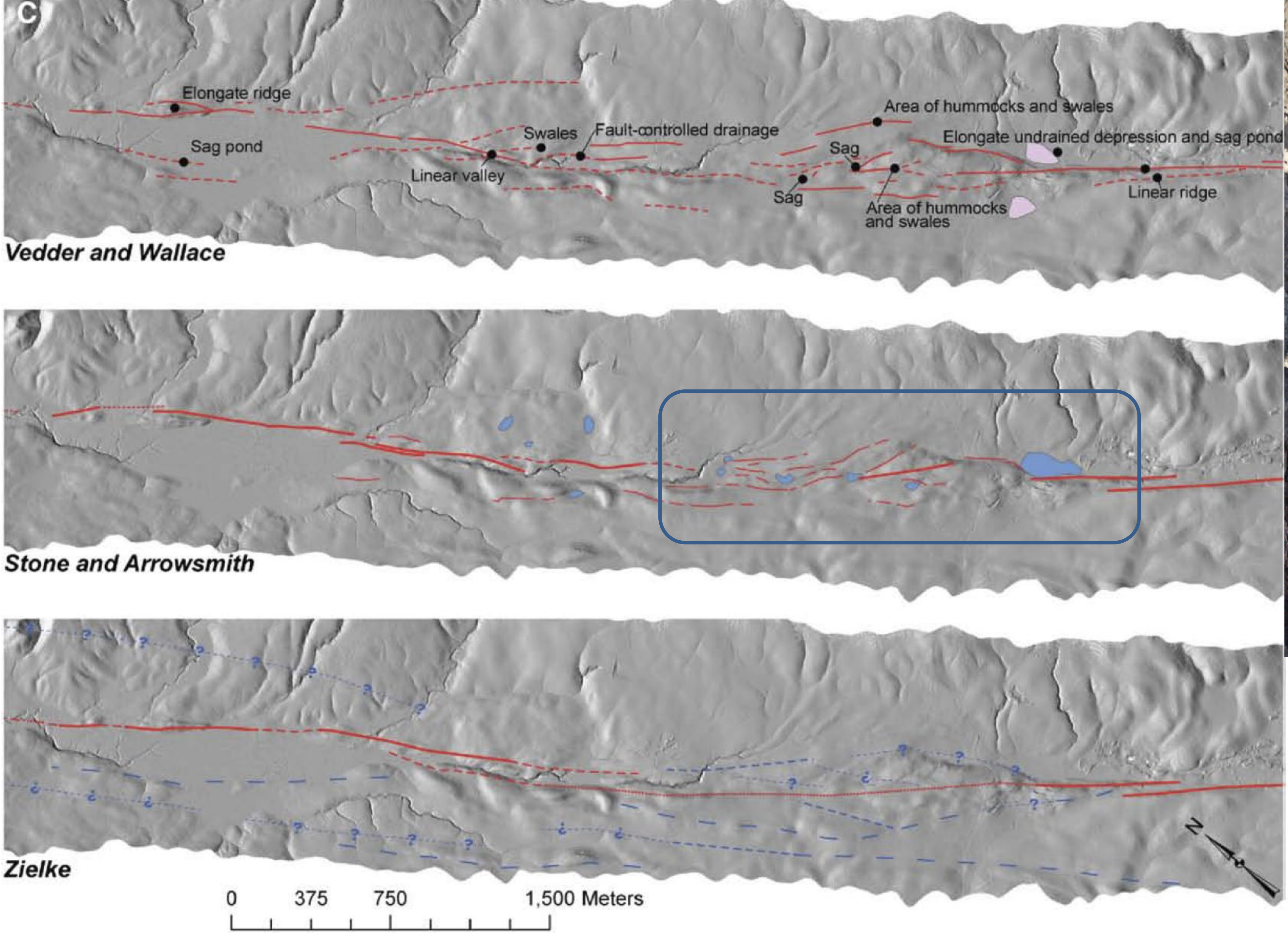

Arrowsmith and Zielke, 2009
Williams in prep.

Northern Carrizo Plain sag ponds; San Andreas Fault

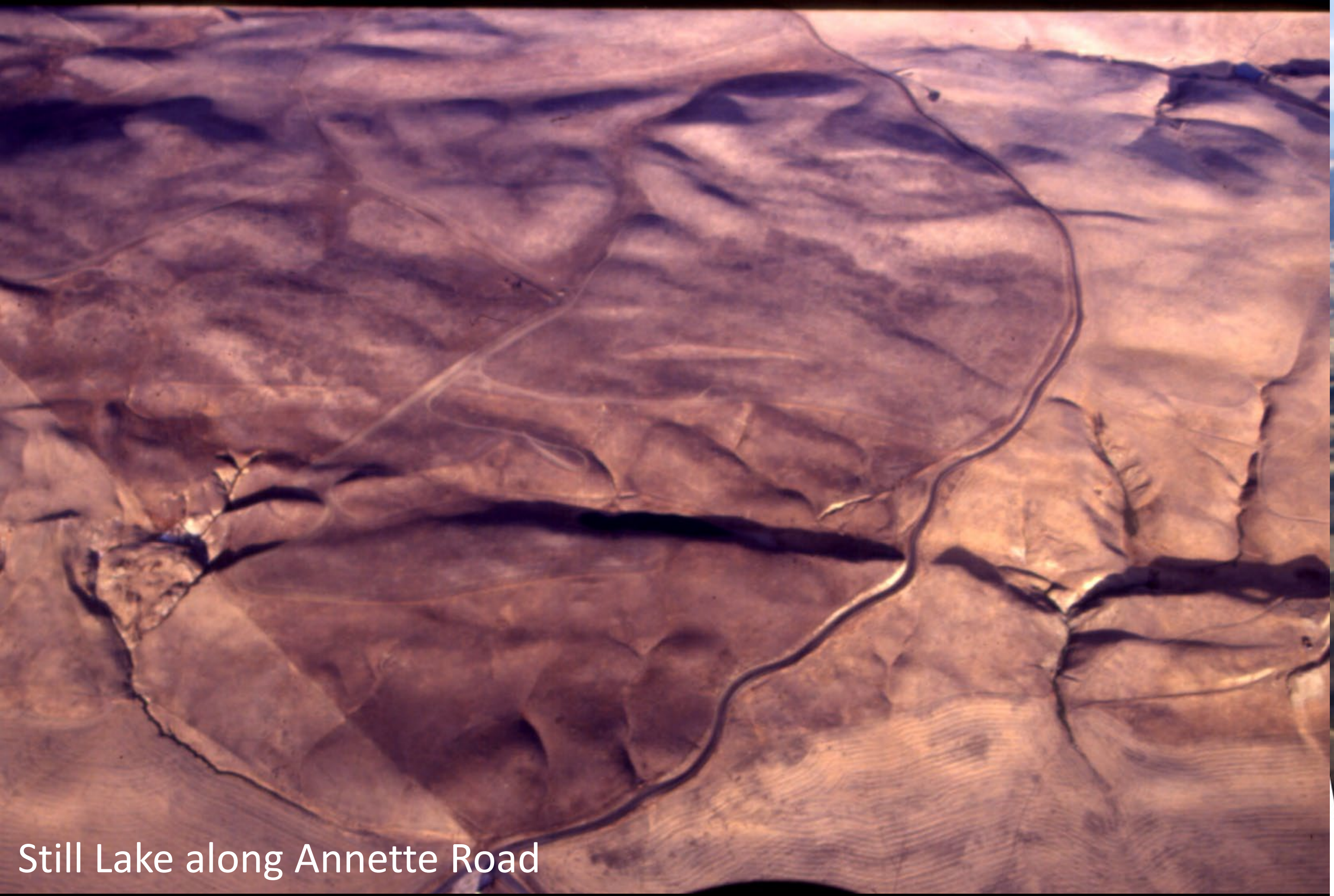

Cholame section of San Andreas Fault

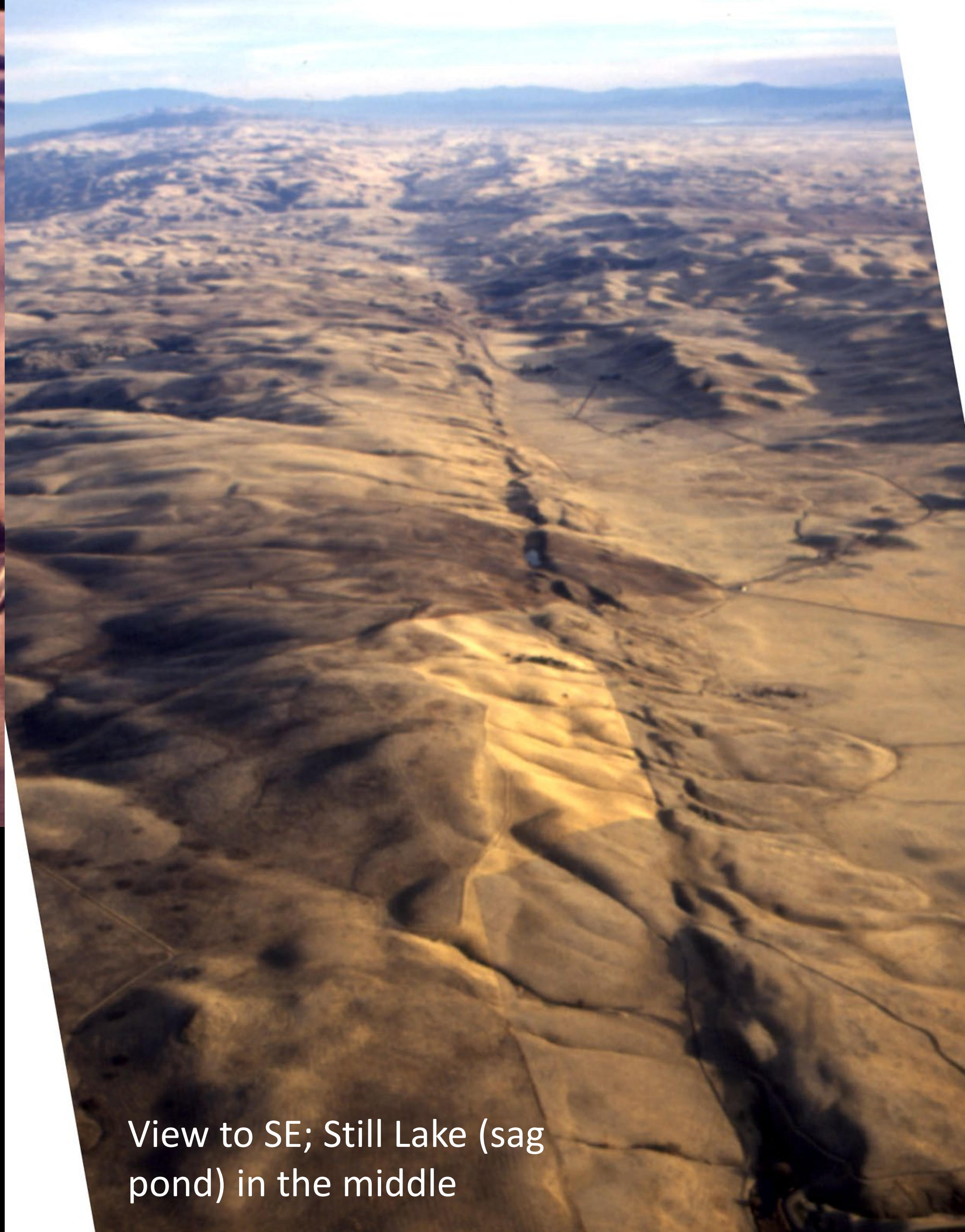

Late Holocene slip rate of the San Andreas fault and its accommodation by creep and moderate-magnitude earthquakes at Parkfield, California

Geology, March 2011; v. 39; no. 3; p. 243–246; doi: 10.1130/G31498.1

Nathan A. Toké[1], J Ramón Arrowsmith[1], Michael J. Rymer[2], Angela Landgraf[3], David E. Haddad[1], Melanie Busch[1], Joshua Coyan[1], and Alexander Hannah[4]

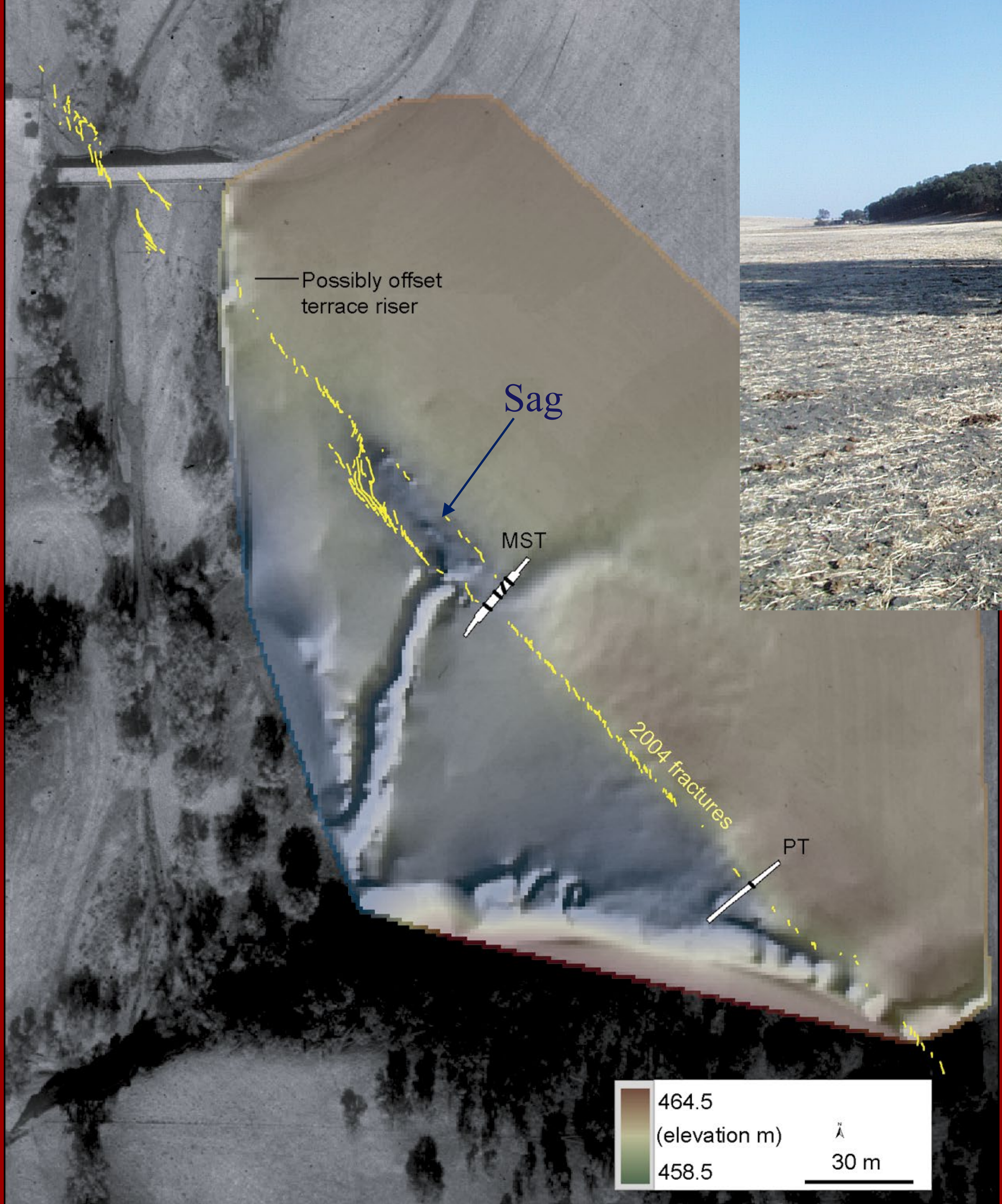

Survey of 369 earthquake fractures in Miller’s field 2 days after the 2004 earthquake:

Spectacular pattern of shearing and association with pre-existing tectonic landforms

Journal of Structural Geology xxx (2013) 1–14
Contents lists available at ScienceDirect
Journal of Structural Geology
journal homepage: www.elsevier.com/locate/jsg

Developing sub 5-m LiDAR DEMs for forested sections of the Alpine and Hope faults, South Island, New Zealand: Implications for structural interpretations

R.M. Langridge [a,*], W.F. Ries [a], T. Farrier [b], N.C. Barth [c], N. Khajavi [d], G.P. De Pascale [d]
[a] Dept. of Active Landscapes, GNS Science, P.O. Box 30-368, Lower Hutt 5010, New Zealand
[b] New Zealand Aerial Mapping, P.O. Box 6, Hastings 4156, New Zealand
[c] Dept. of Geology, University of Otago, P.O. Box 56, Dunedin 9054, New Zealand
[d] Dept. of Geological Sciences, University of Canterbury, P.O. Box 4800, Christchurch 8140, New Zealand

Scale dependence of oblique plate-boundary partitioning: New insights from LiDAR, central Alpine fault, New Zealand

Nicolas C. Barth[1]*, Virginia G. Toy[1], Robert M. Langridge[2], and Richard J. Norris[1]
[1]DEPARTMENT OF GEOLOGY, UNIVERSITY OF OTAGO, P.O. BOX 56, DUNEDIN, NEW ZEALAND
[2]GNS SCIENCE, P.O. BOX 30-368, LOWER HUTT, NEW ZEALAND

LITHOSPHERE; v. 4; no. 5; p. 435–448 | Published online 11 July 2012 | doi: 10.1130/L201.1

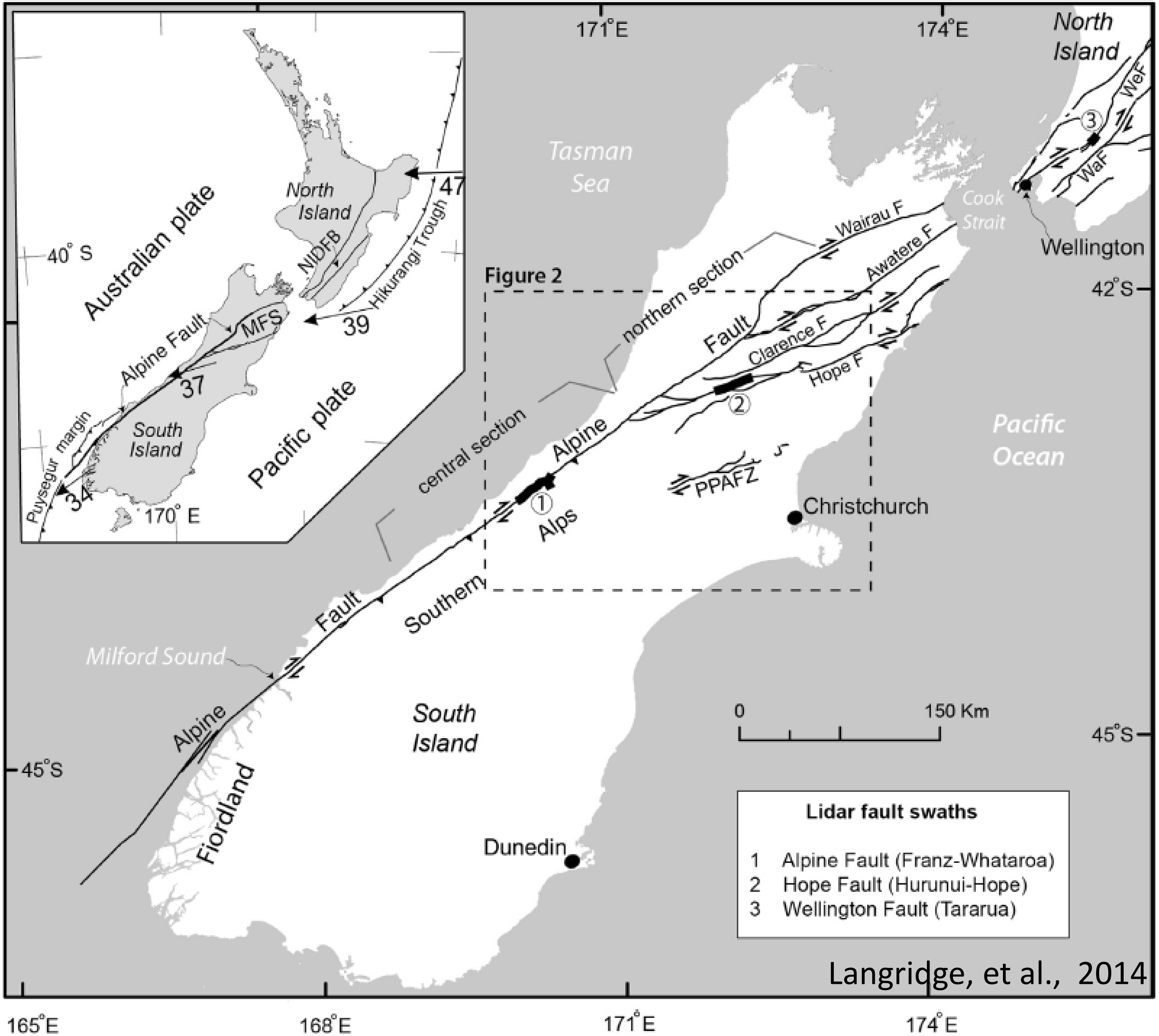

Langridge, et al., 2014

Branch River terraces (Zinke et al., 2021)

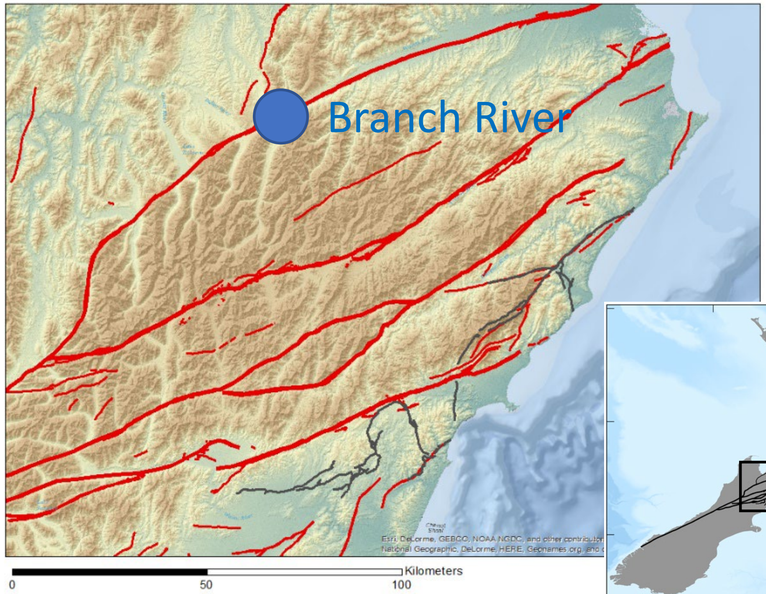

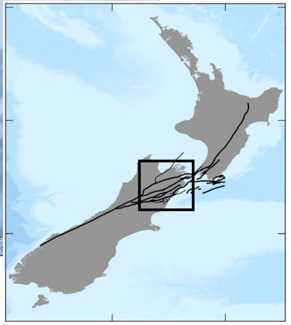

Geomorphic map of terraces at the Branch River site, NZ. Colors delineate topographically (and temporally) distinct terrace treads. Labeling after Lensen (1968).

Terraces are bisected by the Wairau fault (note uncolored fault scarp).

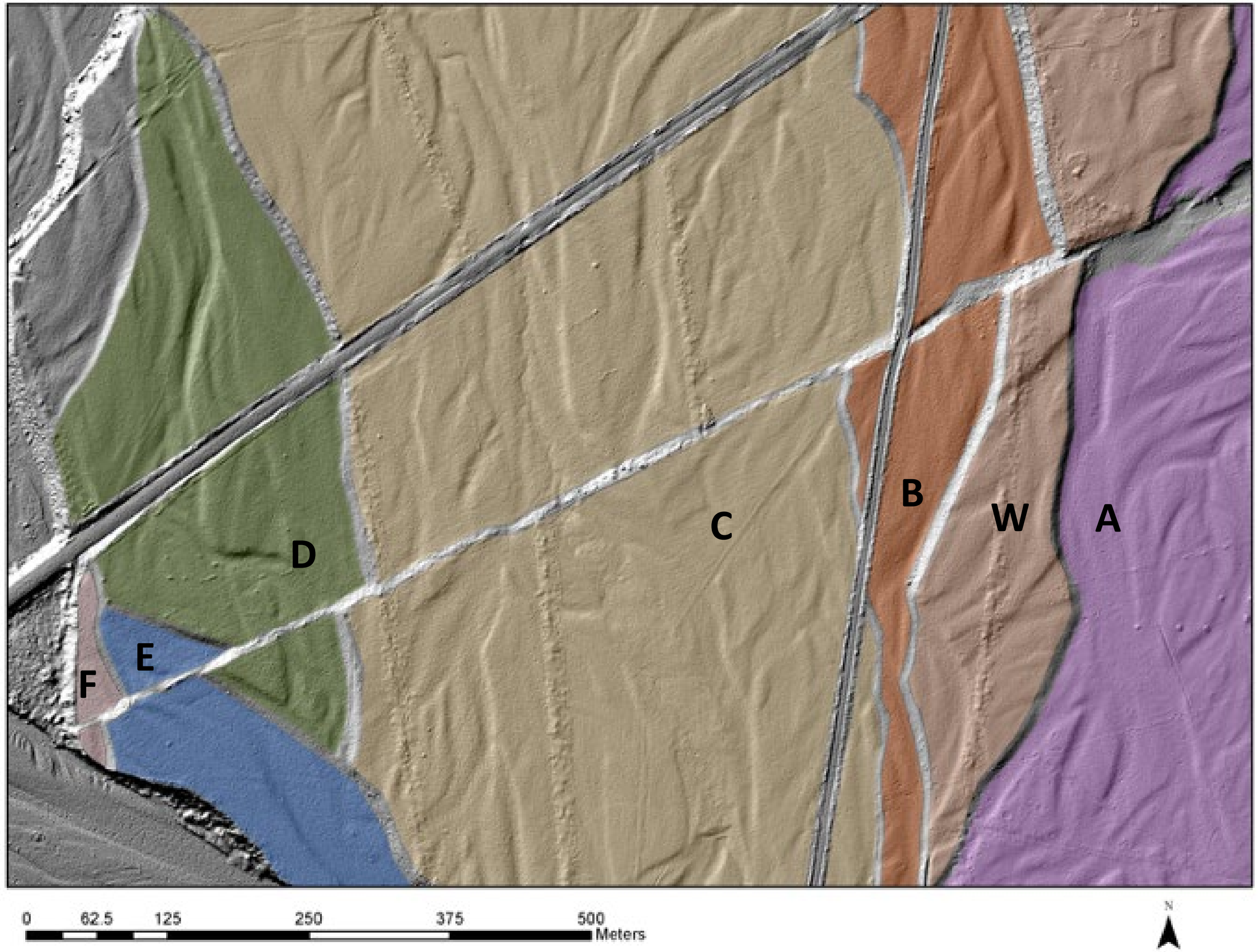

Hope fault Sackungen (Hatem et al., 2020)

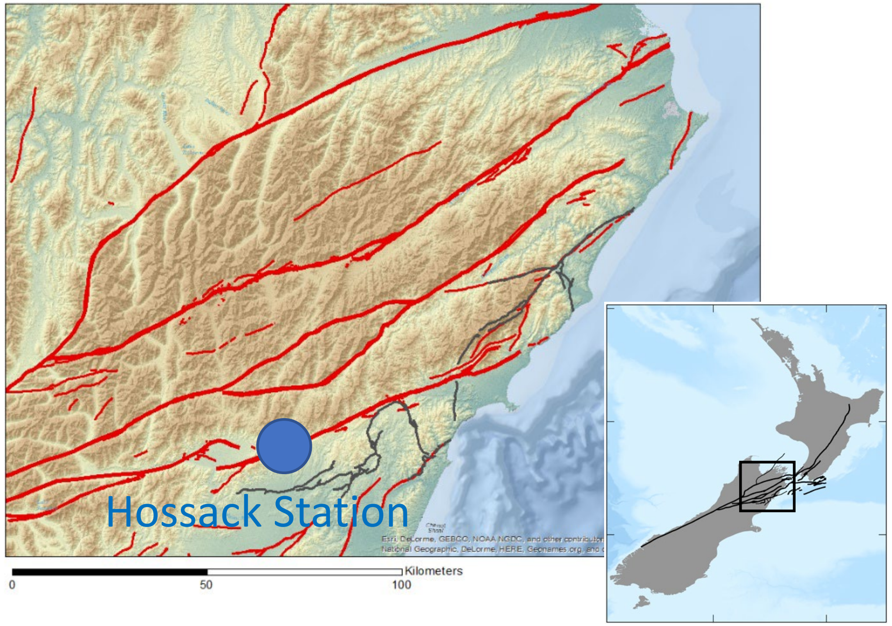

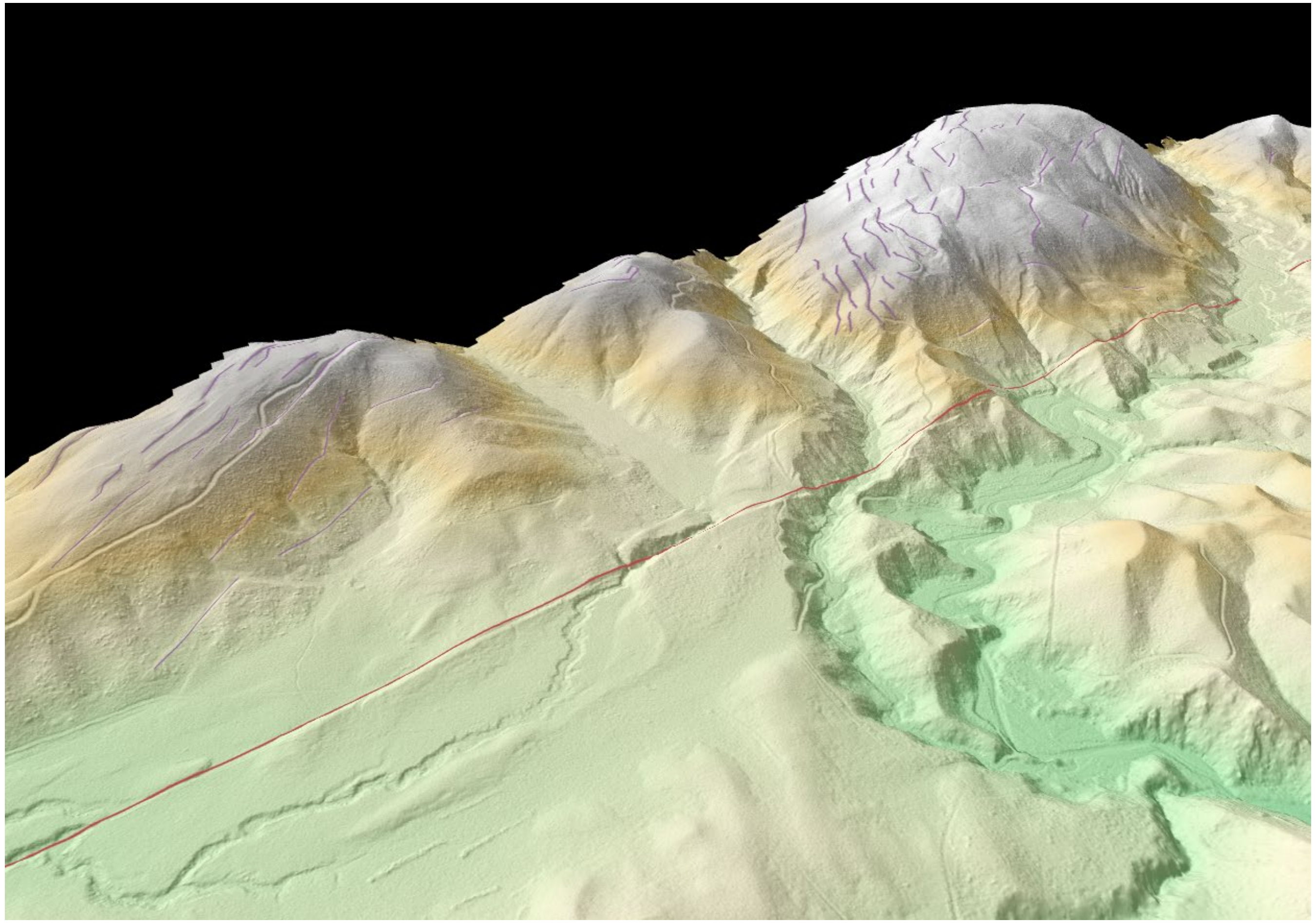

Oblique view of sackungen (purple lines) adjacent to the Hope fault (red line), NZ.


A′
high relief
rangefront
A
Franz
Josef
gravel
floodplain
Waiho
River
Fig. 6
grassland
West Coast
bush cover

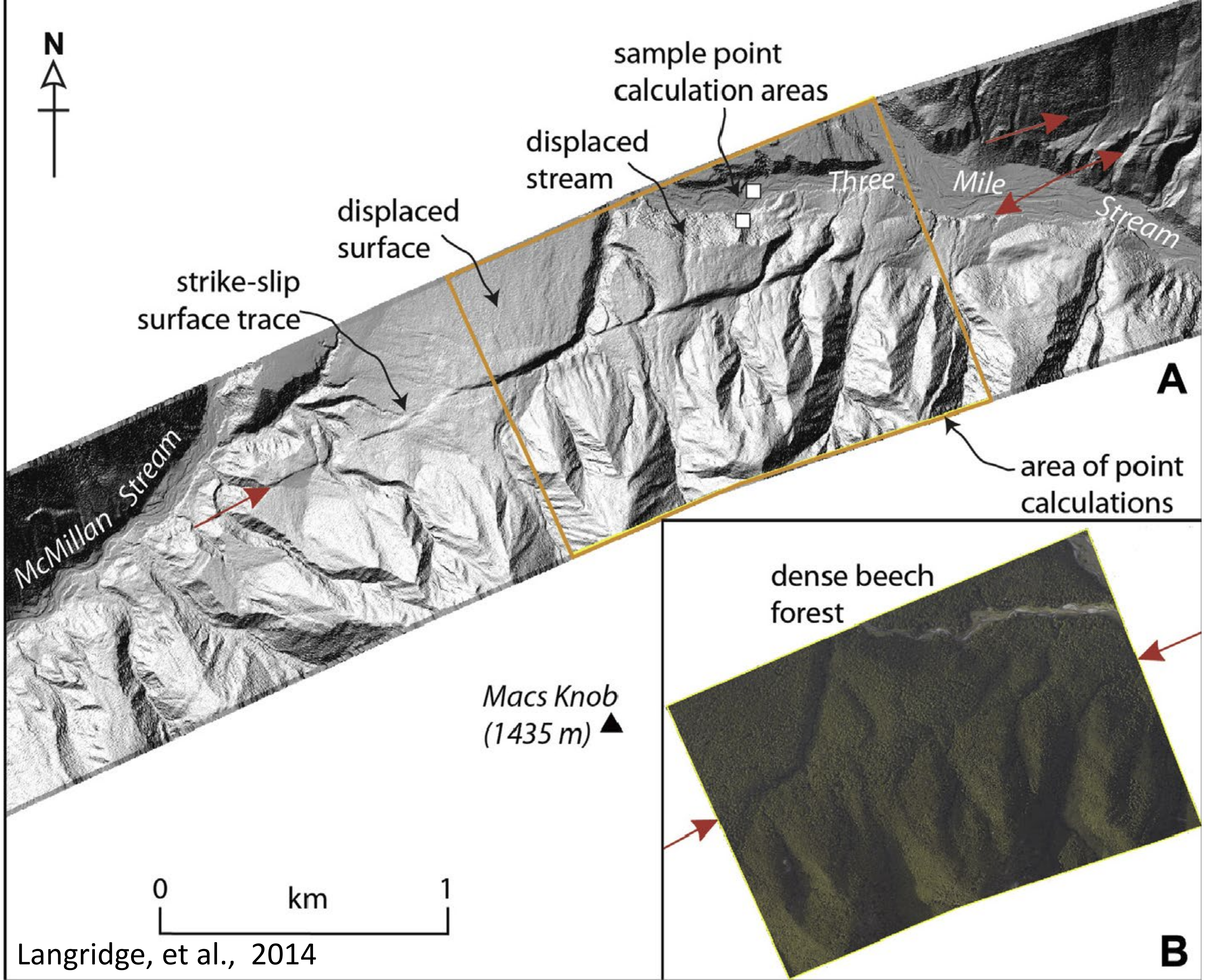

Langridge, et al., 2014

Scale matters

Alpine Fault

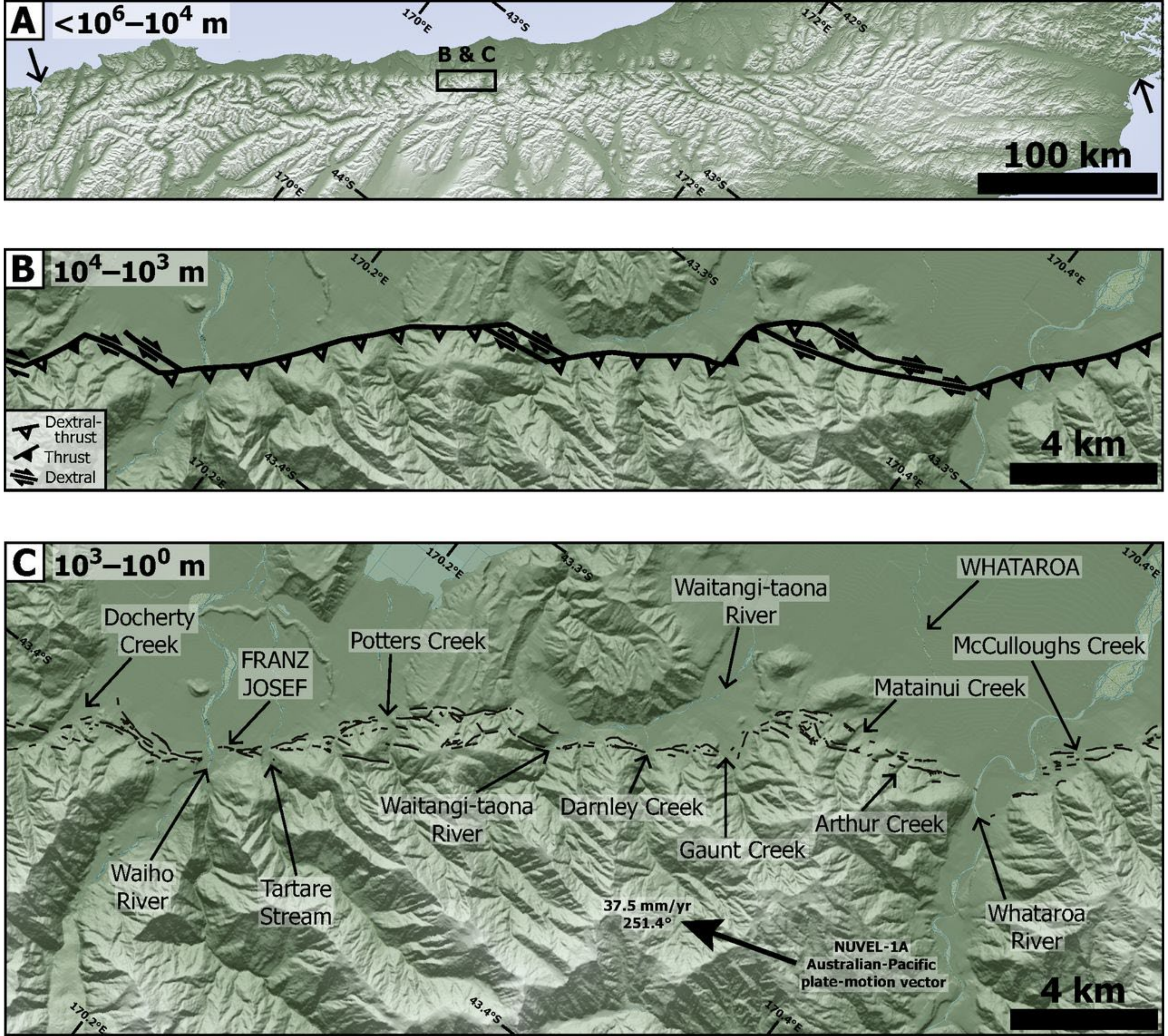

Barth, et al., 2012

Complex structure along ~simple plate boundary fault zone

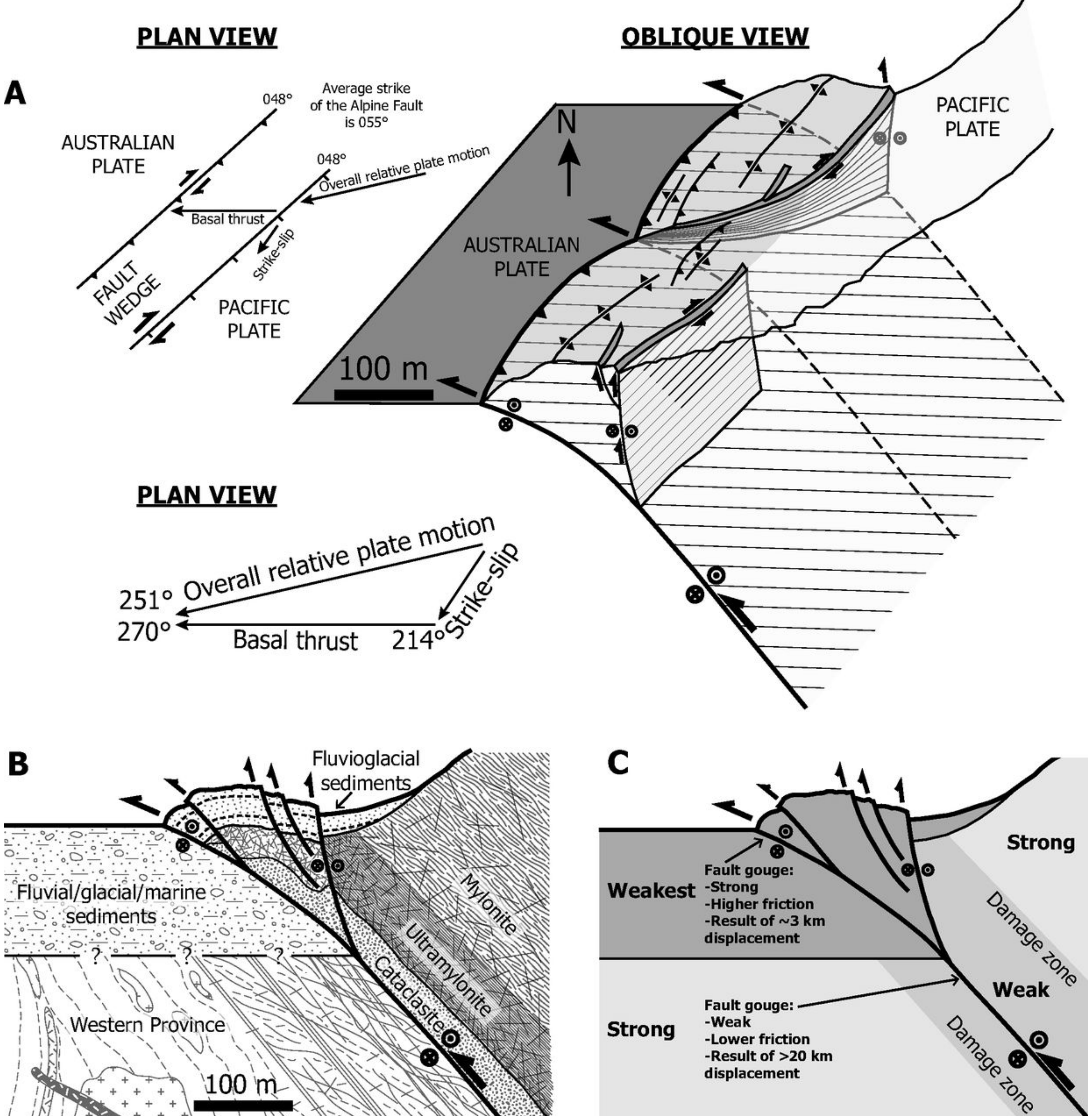

Barth, et al., 2012

Landscape evolution modeling to explore landscape development along strike-slip faults

AGU PUBLICATIONS JGR
Journal of Geophysical Research: Earth Surface

RESEARCH ARTICLE

10.1002/2015JF003618

Dynamic Ridges and Valleys in a Strike-Slip Environment

Alison R. Duvall[1] and Gregory E. Tucker[2]

[1]Department of Earth and Space Sciences, University of Washington, Seattle, Washington, USA, [2]CIRES and Department of Geological Sciences, University of Colorado, Boulder, Colorado, USA

Key Points:
- Strike-slip landscapes are in permanent disequilibrium from river lengthening and capture
- Hillslope ridges upstream of slow-slipping strike-slip faults migrate laterally
- A recognizable suite of geomorphic signatures can indicate horizontal fault slip rate

Abstract Strike-slip faults have long been known for characteristic near-fault landforms such as offset rivers and strike-parallel valleys. In this study, we use a landscape evolution model to investigate the longer-term, catchment-wide landscape response to horizontal fault motion. Our results show that strike-slip faulting induces a persistent state of disequilibrium in the modeled landscapes brought about by river

JGR Solid Earth

RESEARCH ARTICLE

10.1029/2019JB018596

Offset Channels May Not Accurately Record Strike-Slip Fault Displacement: Evidence From Landscape Evolution Models

Nadine G. Reitman[1], Karl J. Mueller[1], Gregory E. Tucker[1,2], Ryan D. Gold[3], Richard W. Briggs[3], and Katherine R. Barnhart[1,2]

[1]Department of Geological Sciences, University of Colorado Boulder, Boulder, CO, USA, [2]Cooperative Institute for Research in Environmental Sciences (CIRES), University of Colorado Boulder, Boulder, CO, USA, [3]Geologic Hazards Science Center, U.S. Geological Survey, Golden, CO, USA

Key Points:
- Mean-measured offset records modeled slip only if fault zone width is <5 m, total slip is less than channel spacing, and short time since earthquake
- Postearthquake landscape evolution widens the geomorphic fault zone and smears out initially discrete channel offsets
- Offset measurements have ~30% natural variability, but modeled slip is recovered by taking the mean of multiple offset measurements

Abstract Slip distribution, slip rate, and slip per event for strike-slip faults are commonly determined by correlating offset stream channels—under the assumption that they record seismic slip—but offset

THE GEOLOGICAL SOCIETY OF AMERICA®

GEOLOGY, January 2018; v. 46; no. 1; p. 59–62 | Data Repository item 2018013 | https://doi.org/10.1130/G39820.1 | Published online 29 November 2017

Off-fault deformation rate along the southern San Andreas fault at Mecca Hills, southern California, inferred from landscape modeling of curved drainages

Harrison J. Gray[1], Charles M. Shobe[1], Daniel E.J. Hobley[2], Gregory E. Tucker[1], Alison R. Duvall[3], Sarah A. Harbert[3], and Lewis A. Owen[4]

[1]Cooperative Institute for Research in Environmental Sciences (CIRES) and Department of Geological Sciences, University of Colorado, Boulder, Colorado 80309, USA
[2]School of Earth and Ocean Sciences, Cardiff University, Cardiff CF10 3AT, UK
[3]Department of Earth and Space Sciences, University of Washington, Seattle, Washington 98195, USA
[4]Department of Geology, University of Cincinnati, Cincinnati, Ohio 45221, USA

2.1. Landscape Evolution Model Setup

The landscape evolution model follows the models of Duvall and Tucker (2015) and Gray et al. (2018). Landscape evolution and strike-slip displacement are based on the following equation:

$$\frac{\partial z}{\partial t} = U - V(y)\frac{\partial z}{\partial x} - \left(KA^{1/2}S - E_{crit}\right) + D\nabla^2 z, \quad (1)$$

where z is height of the landscape (m), t is time (year), x is fault-parallel direction (m), y is fault-perpendicular direction (m), U is relative rock uplift (m/yr), $V(y)$ is time-averaged lateral displacement rate (m/year), K is erodibility (year^{-1}), A is drainage area (m^2), S is slope gradient (positive downward), E_{crit} is a threshold on stream power (m^2/year), and D is hillslope diffusivity coefficient (m^2/year). The reader is referred to Duvall and Tucker (2015) for full definition and nondimensionalization of the landscape evolution model. The only modification is in the lateral displacement term because in Duvall and Tucker (2015)

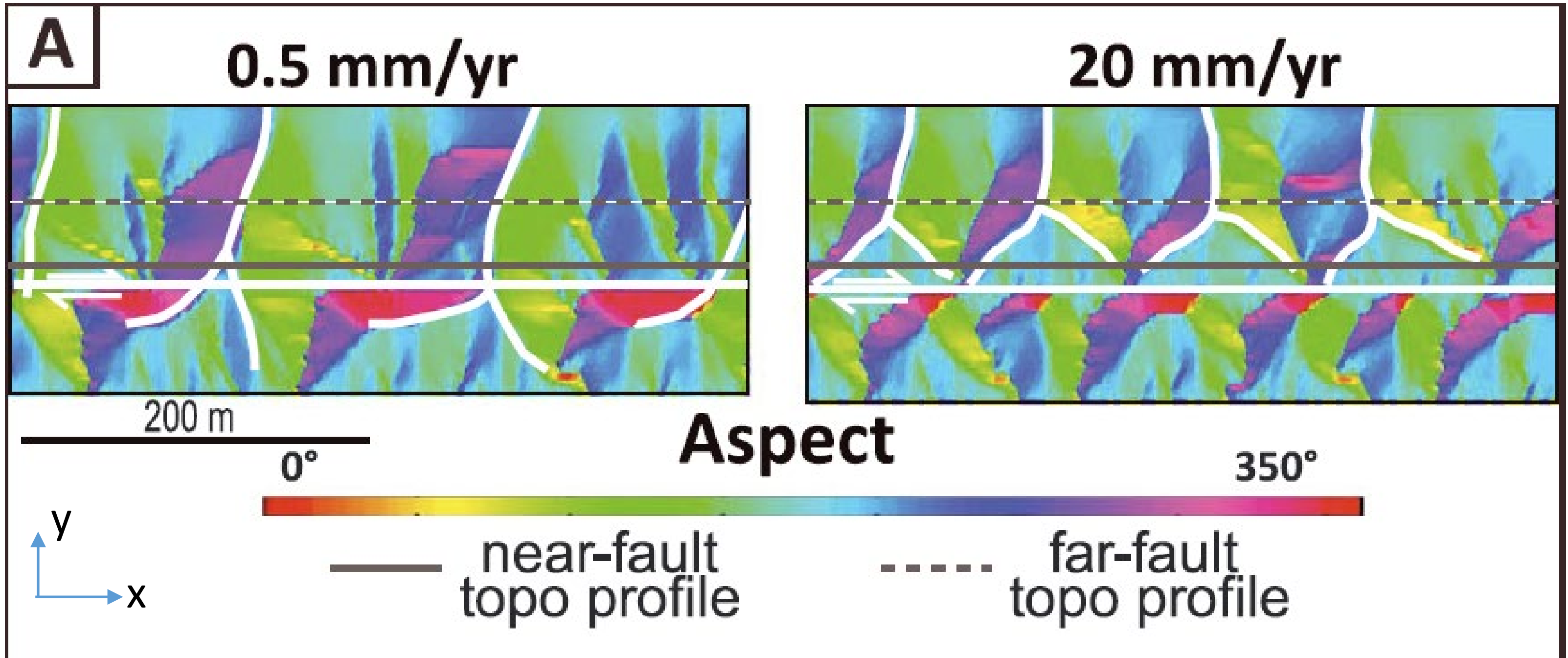

Duvall and Tucker, 2015

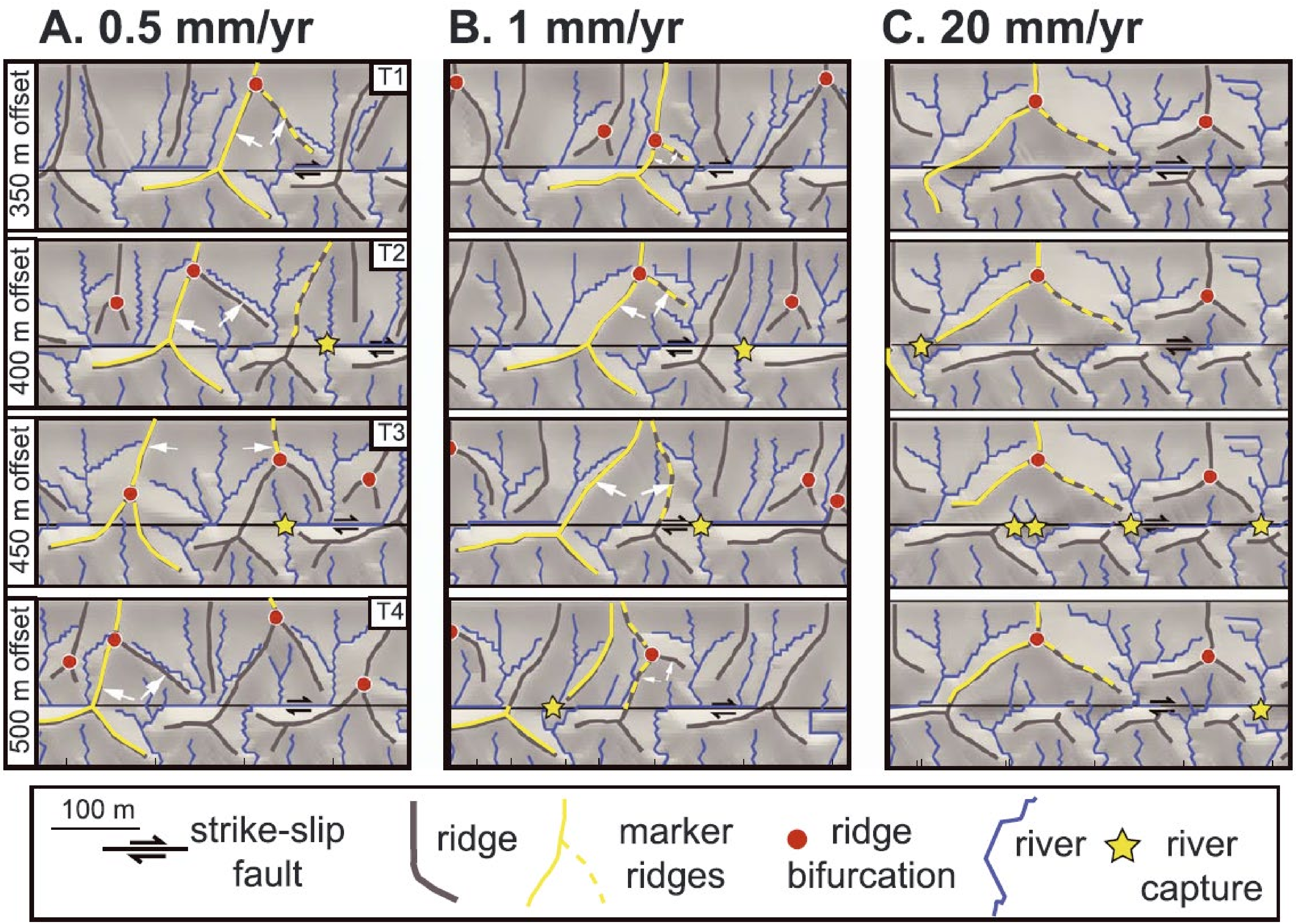

Summary

- Slip rate relative to surface process rates
- Localization ~ slip rate and scale of mapping
- Fault zone discontinuities
- Fault zone orientation relative to drainage network (parallel or perpendicular)
- Degree of (differential) rock uplift along the fault zone: can inset the landscape

Strike-slip faults

Ramón Arrowsmith

ramon.arrowsmith@asu.edu

School of Earth and Space Exploration
Arizona State University

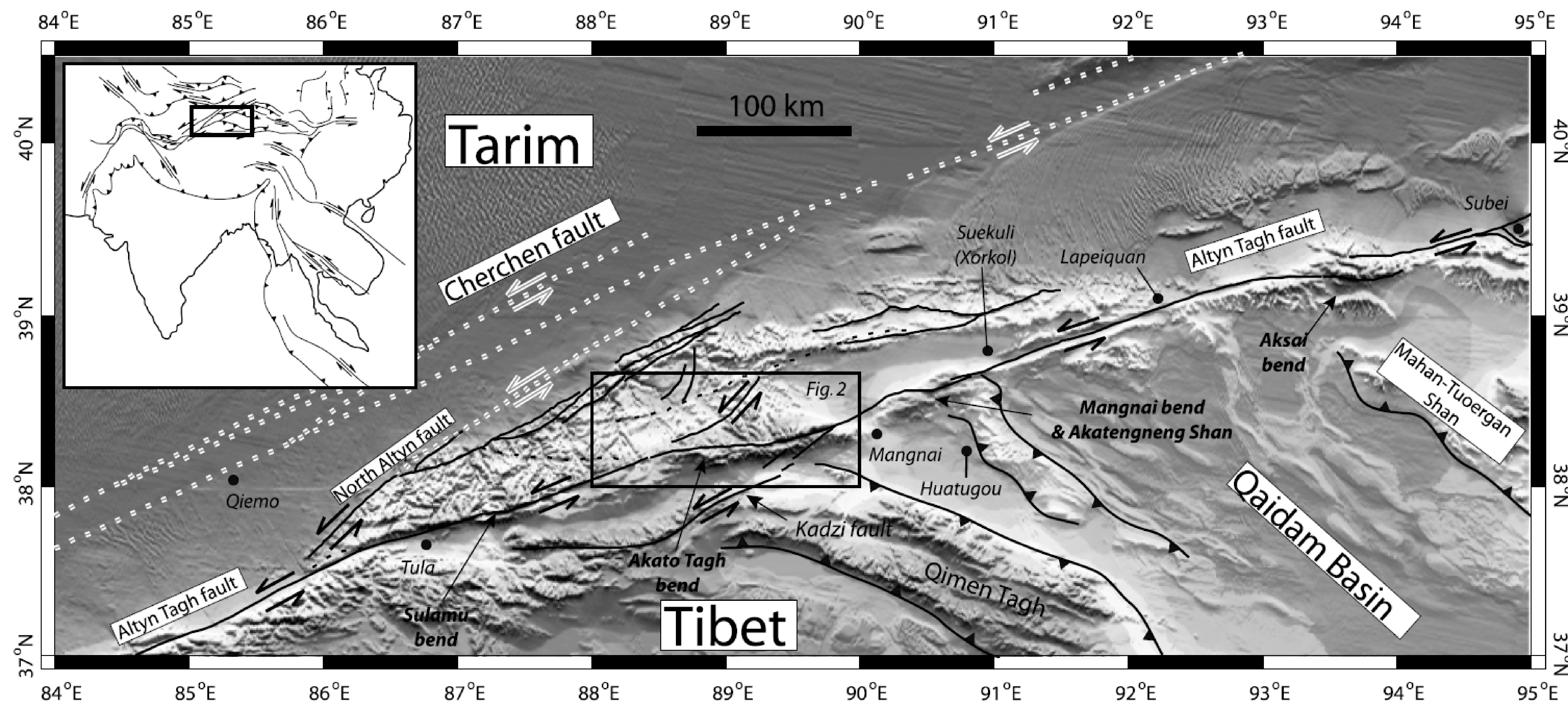

Altyn Tagh Fault, western China (Cowgill, et al., 2004)

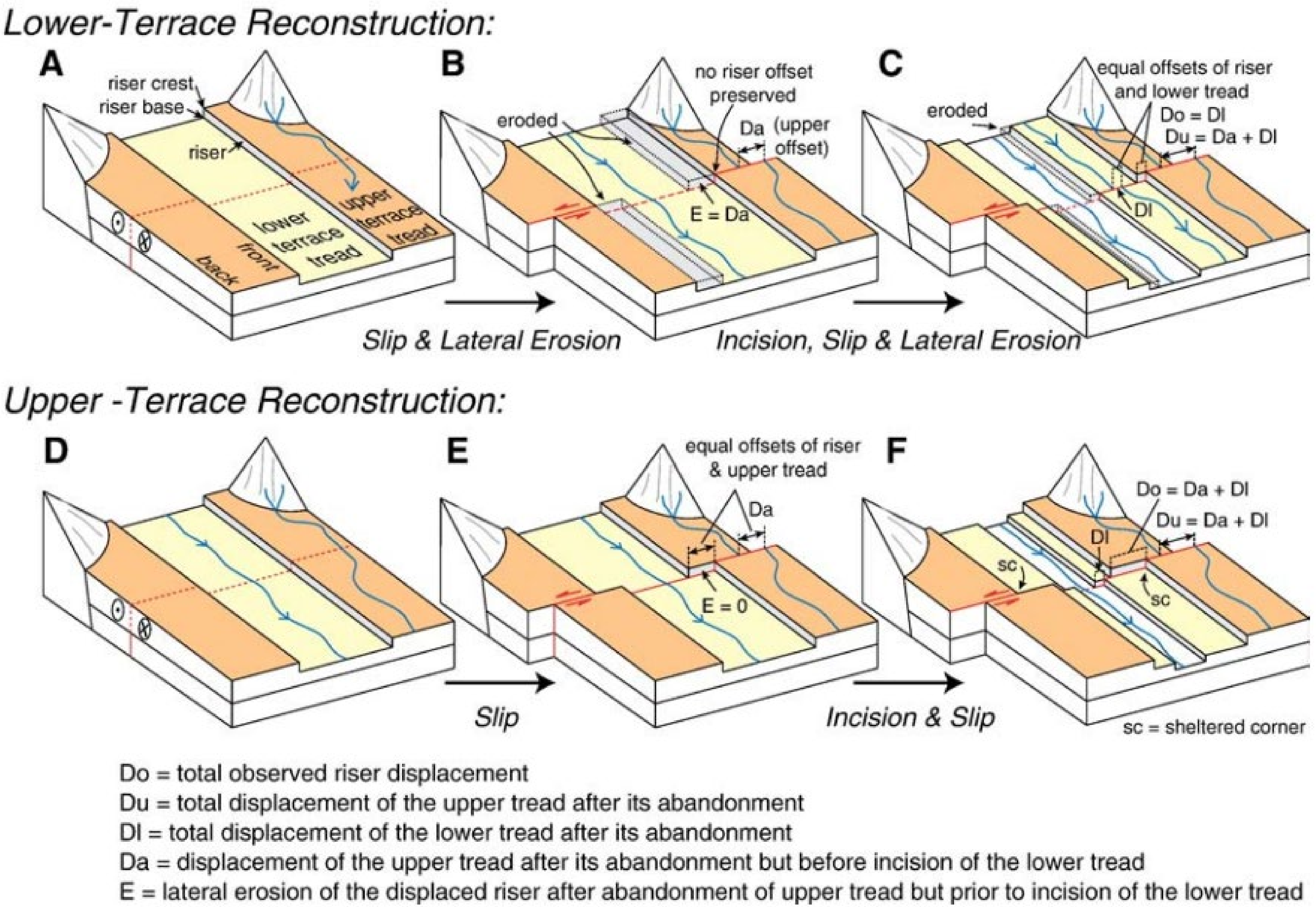

Cowgill, EPSL, 2007

JOURNAL OF GEOPHYSICAL RESEARCH, VOL. 114, B04401, doi:10.1029/2008JB005913, 2009

Riser diachroneity, lateral erosion, and uncertainty in rates of strike-slip faulting: A case study from Tuzidun along the Altyn Tagh Fault, NW China

Ryan D. Gold,[1] Eric Cowgill,[1] J Ramón Arrowsmith,[2] John Gosse,[3] Xuanhua Chen,[4] and Xiao-Feng Wang[4]

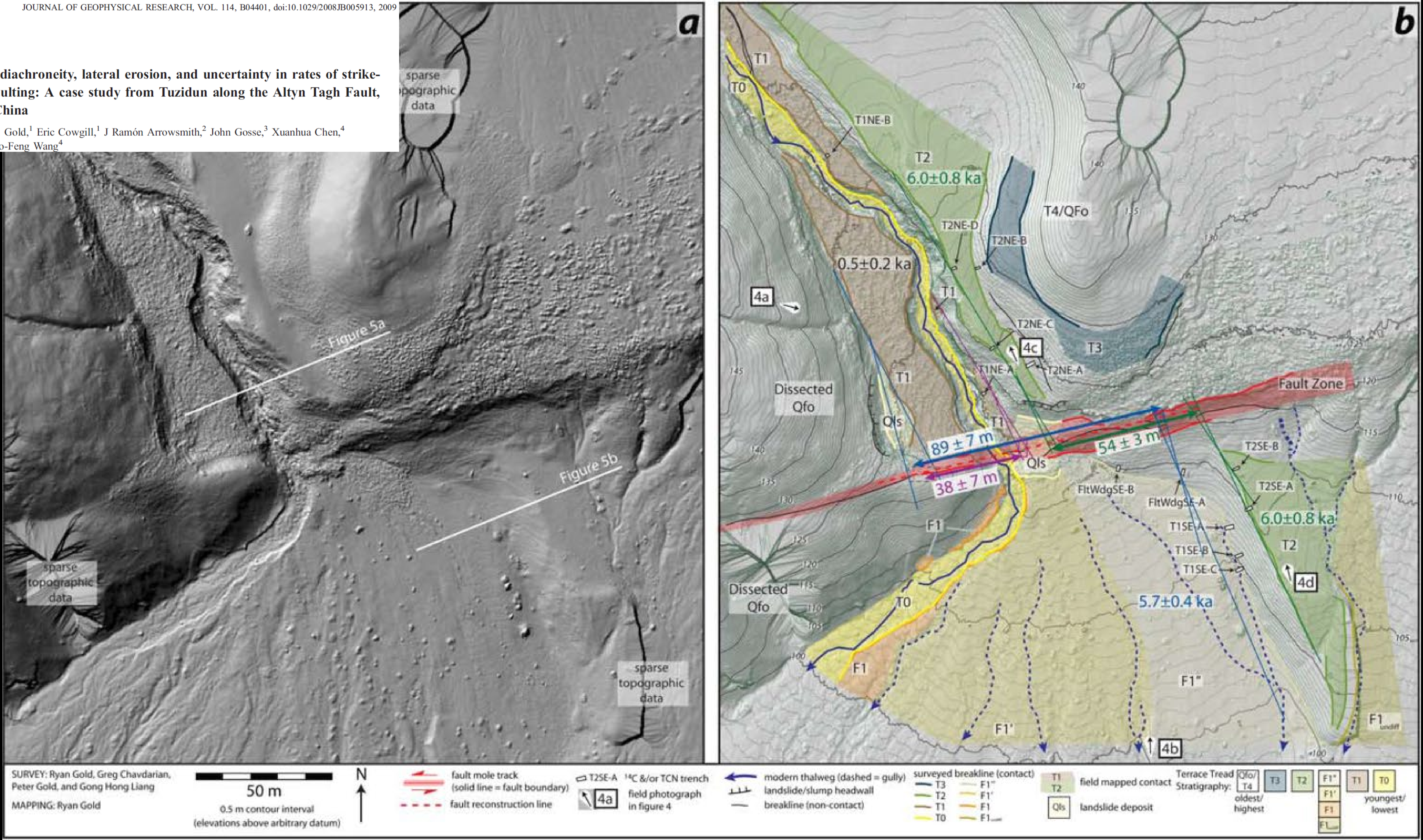

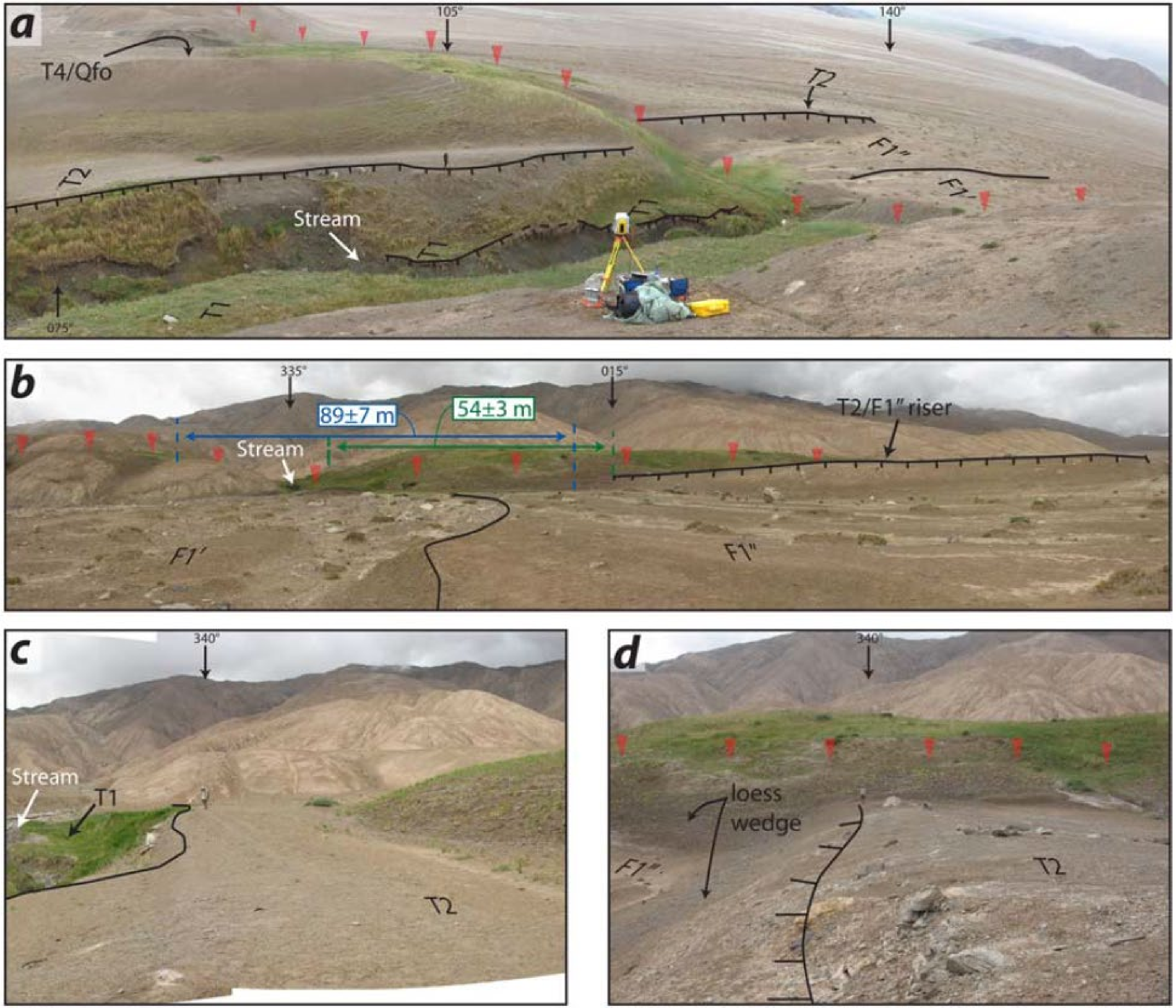

a
105°
140°
T4/Qfo
T2
T2
F1''
F1'
Stream
T1
075°
b
335°
015°
89±7 m
54±3 m
Stream
T2/F1'' riser
F1'
F1''
c
340°
Stream
T1
T2
d
340°
loess
wedge
F1''
T2

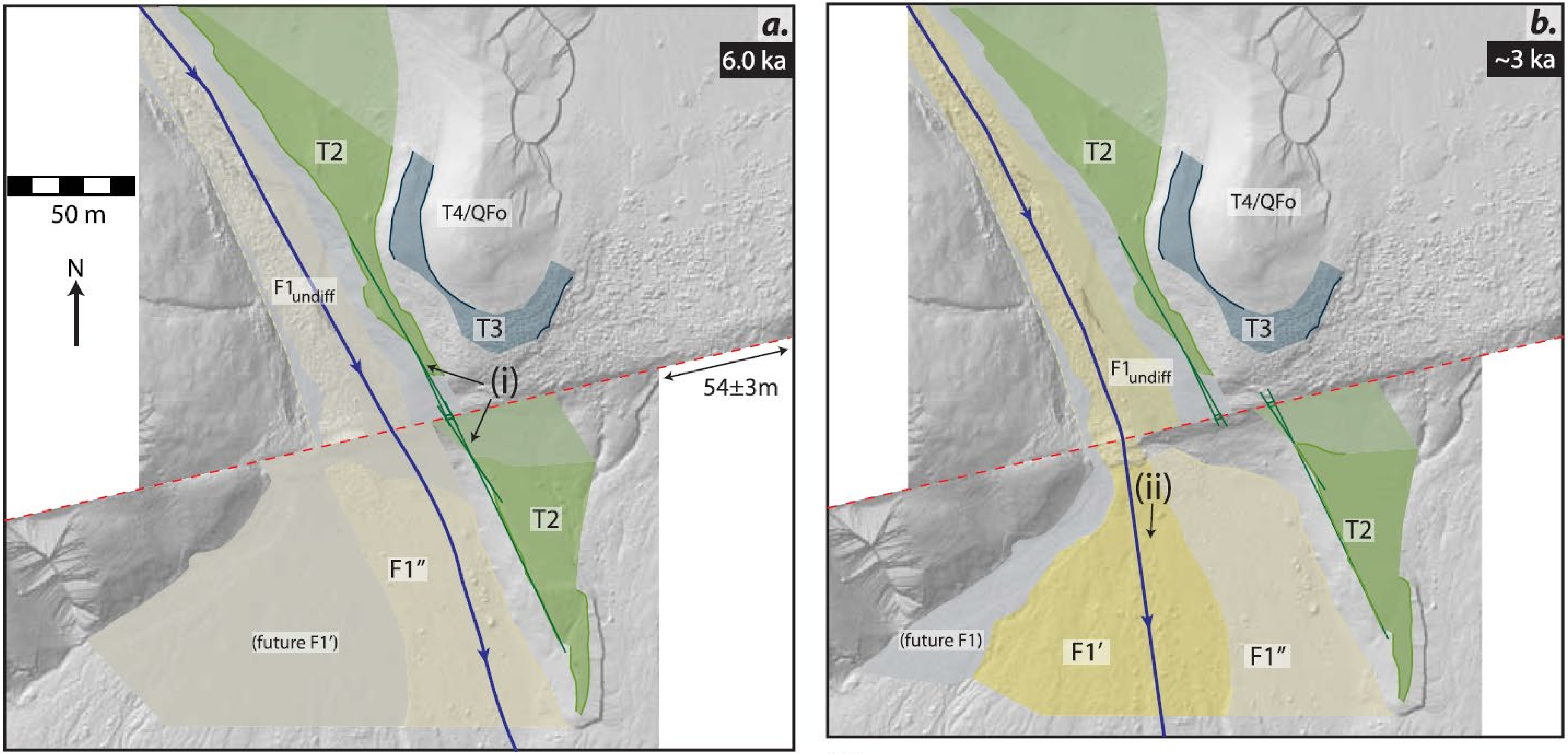

(i) Downstream T2/F1″ and upstream T2/$F1_{undiff}$ riser crests formed and experience no further lateral erosion.

(ii) F1′ lobe deposited

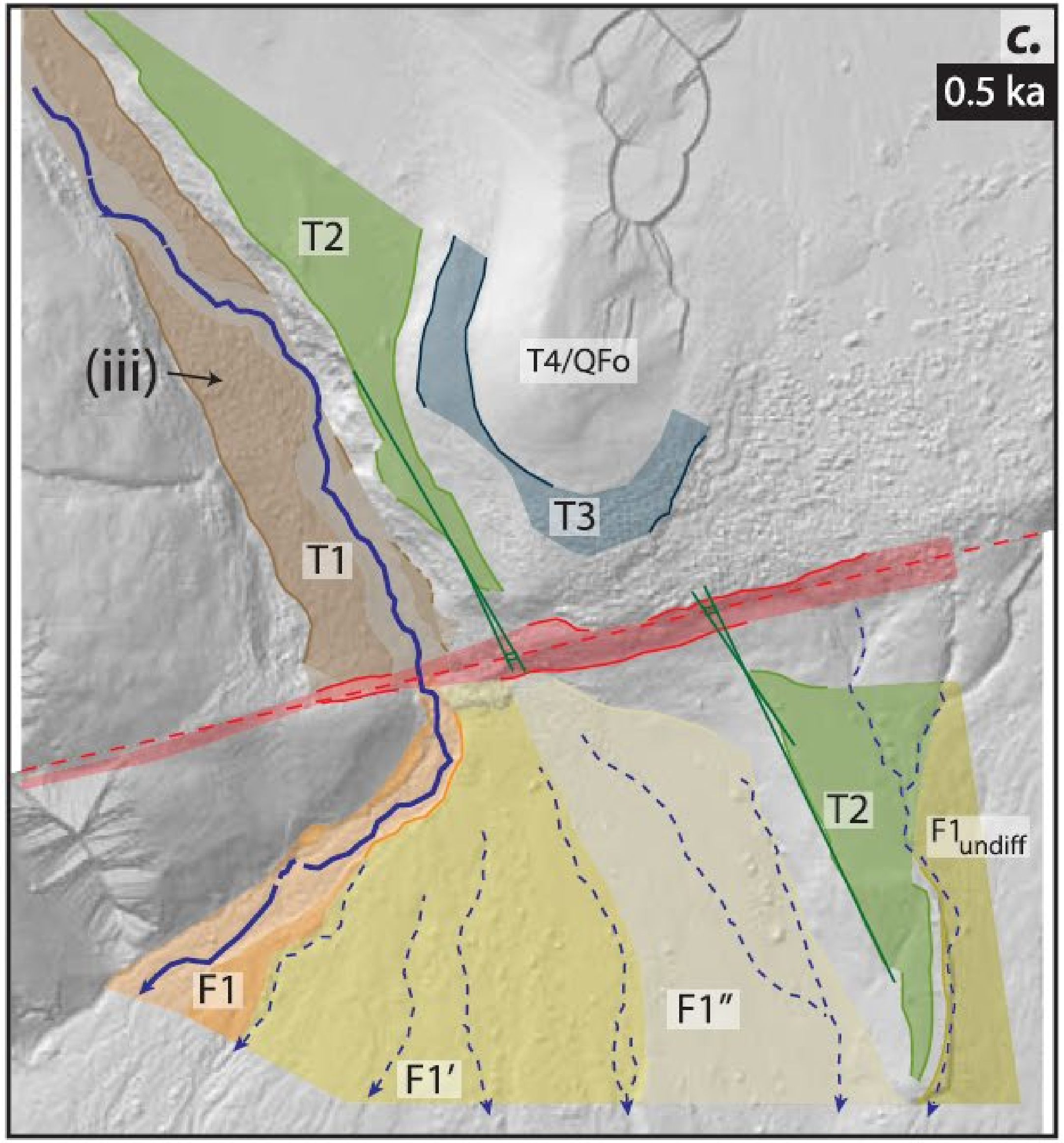

(iii) T1 deposited and abandoned.

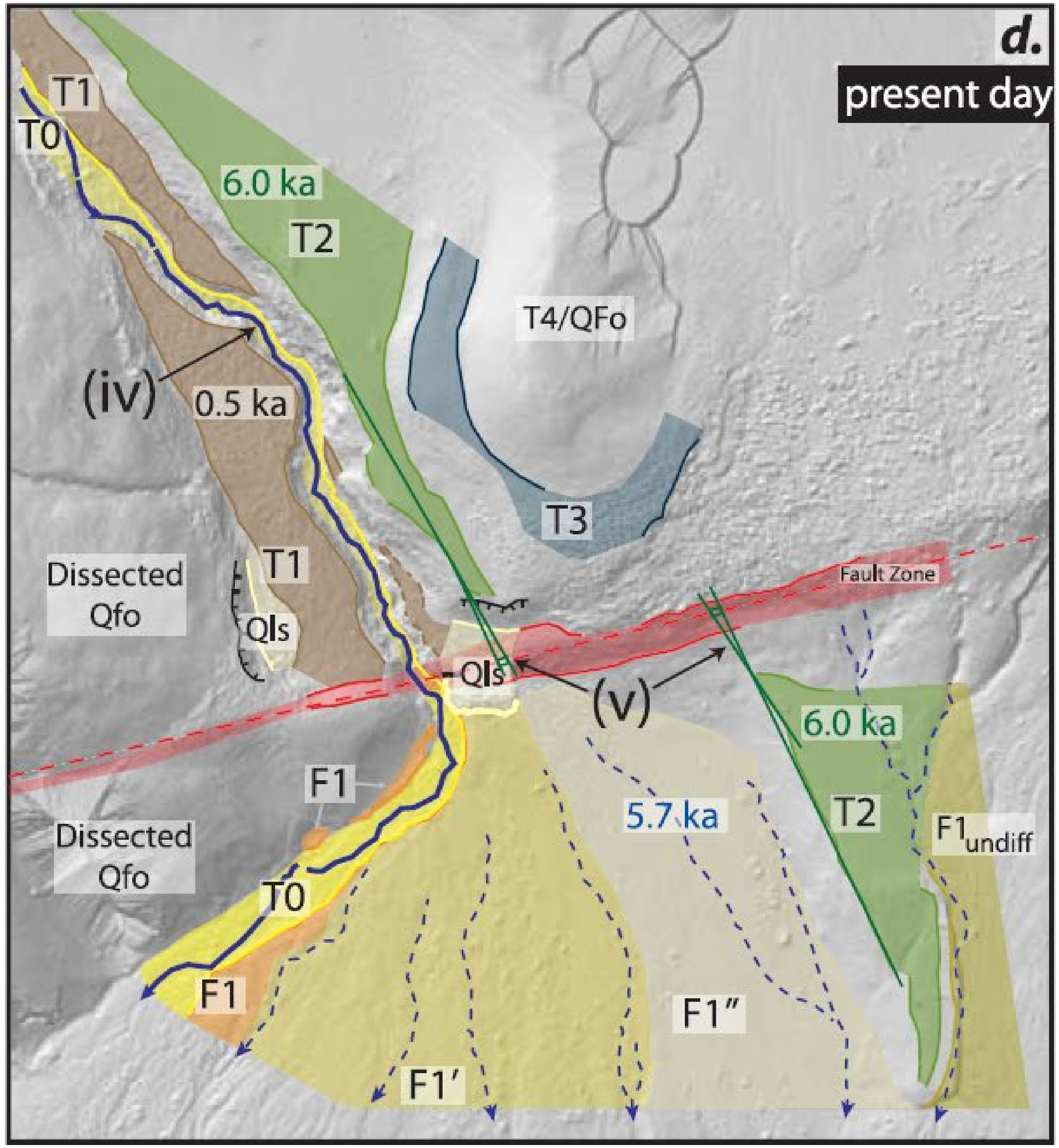

(iv) T0 deposited and occupied.

(v) Maximum of 54 ± 3 m of displacement since abandonment of the T2 surface at 6.0 ± 0.8 ka. Yields a minimum slip-rate of 9.0 ± 1.3 mm/yr.

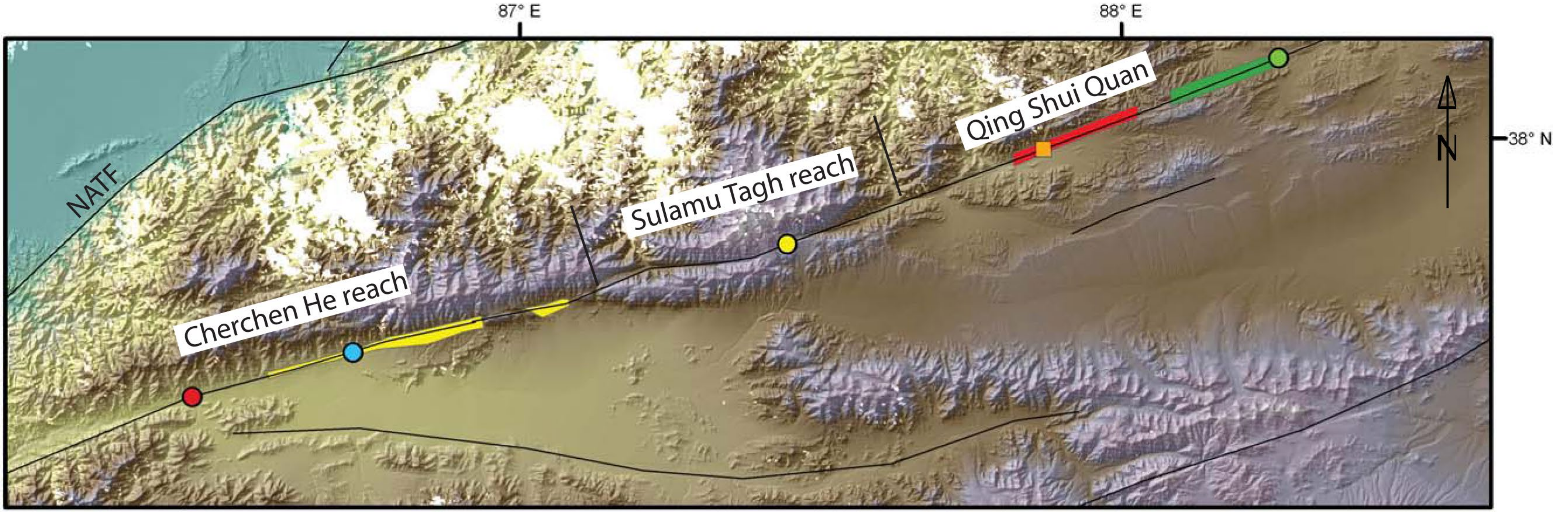

Active fault trace

Digital Globe coverage

Cherchen He field area

Central field area

Cold Water Springs field area

Cowgill et al., in press

Gold R., in press

Meriaux et al., 2004

Gold et al., in press

Meriaux et al., 2004: Cowgill et al., 2007

Summer 2012 Field work: Cherchen He and Qing Shui Quan

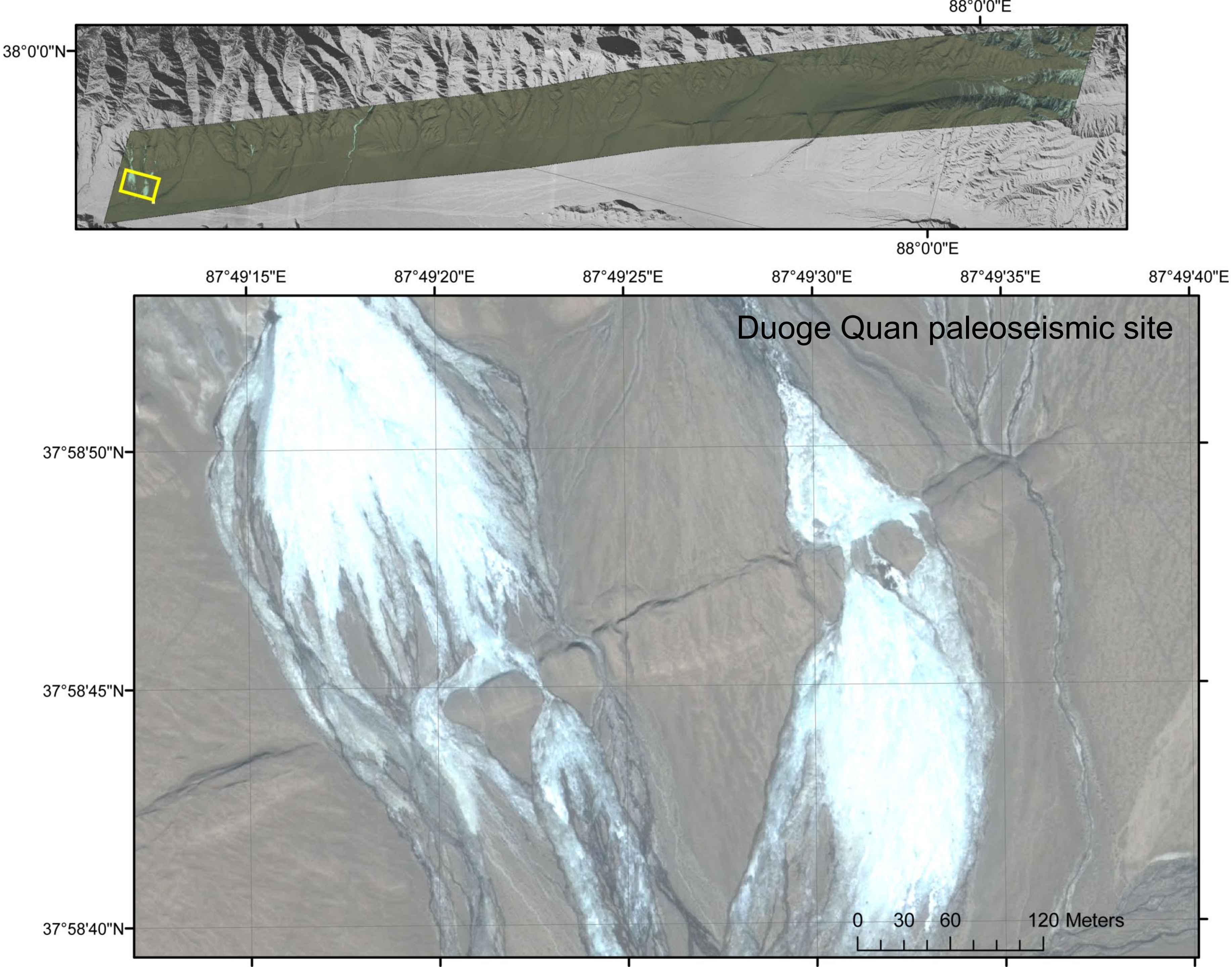

88°0'0"E
38°0'0"N
88°0'0"E
87°49'15"E
87°49'20"E
87°49'25"E
87°49'30"E
87°49'35"E
87°49'40"E
Duoge Quan paleoseismic site
37°58'50"N
37°58'45"N
37°58'40"N
0 30 60 120 Meters

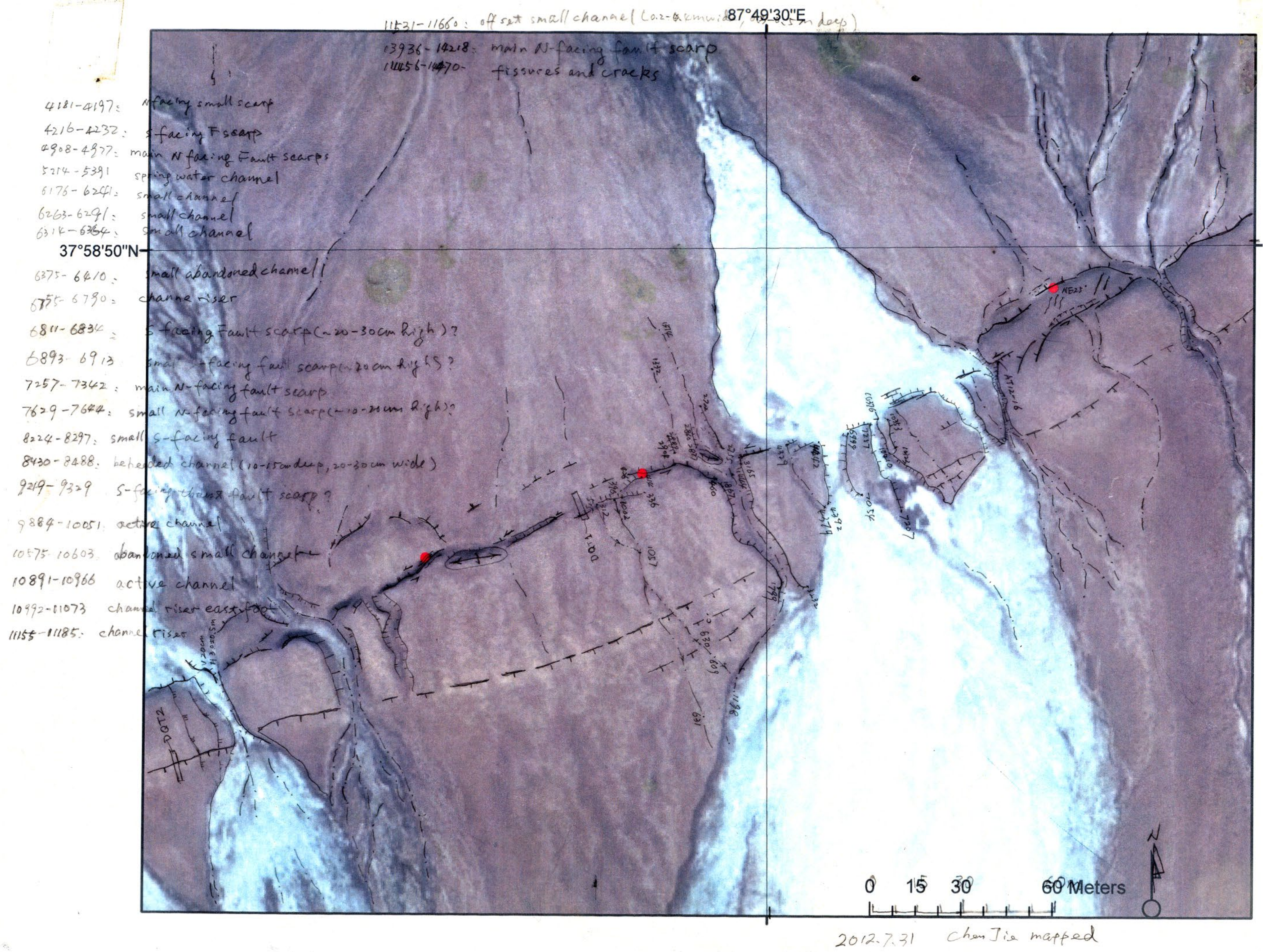
11531-11660: offset small channel
13936-14218: main N-facing fault scarp
11456-11470: fissures and cracks
87°49'30"E
4181-4197: N facing small scarp
4216-4232: S facing F scarp
4908-4977: main N facing Fault scarps
5214-5391 spring water channel
6176-6241: small channel
6263-6291: small channel
6314-6364: small channel
37°58'50"N
6375-6410: small abandoned channel
6755-6790: channel riser
6811-6834: S facing Fault scarp (~20-30cm high)?
6893-6913 small S facing fault scarp (~20cm high)?
7257-7342: main N-facing fault scarp
7629-7644: small N-facing fault scarp (~10-20cm high)?
8224-8297: small S-facing fault
8430-8488: beheaded channel (10-15cm deep, 20-30cm wide)
9219-9329 S-facing thrust fault scarp?
9884-10051 active channel
10575-10603 abandoned small channel
10891-10966 active channel
10992-11073 channel riser east foot
11155-11185 channel riser
0 15 30 60 Meters
N
2012.7.31 Chen Jie mapped

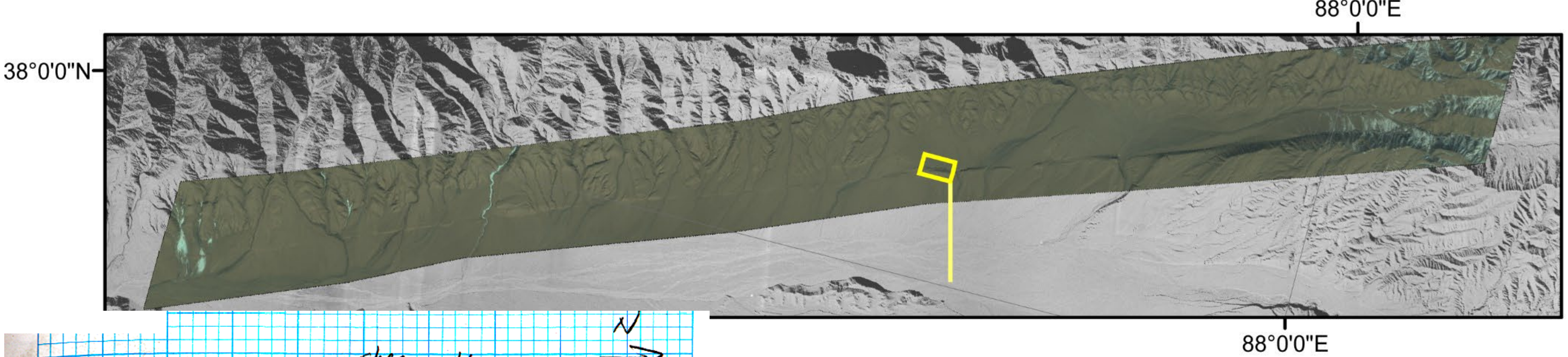
88°0'0"E
38°0'0"N
88°0'0"E

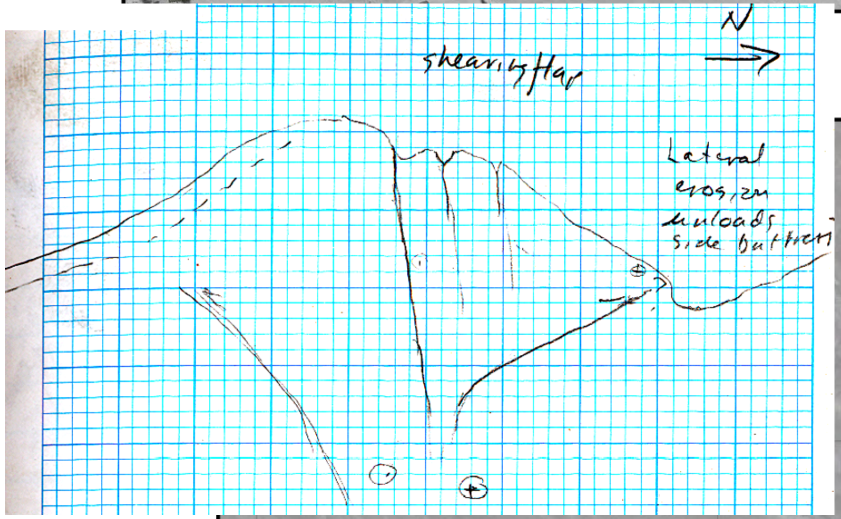
N
shearing flap
Lateral
erosion
unloads
side buttress


87°56'20"E
87°56'25"E
"Structural Geology" site
73007JRA-E
38°0'50"N

Cowgill trace mapping